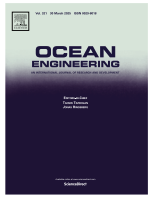
Ocean Engineering 356 (2026) 125239



Contents lists available at ScienceDirect

Ocean Engineering

journal homepage: www.elsevier.com/locate/oceaneng



Research paper



Traveling wave dynamics in higher-order nonlinear Klein–Gordon equations

Asıf Yokus [a], Muhammad Abubakar Isah [b,*], Doğan Kaya [c]

[a] Faculty of Science, Department of Mathematics, Firat University, Elazig, Turkey
[b] Department of Mathematics, Istanbul Ticaret University, 34445, Istanbul, Turkey
[c] Faculty of Engineering Department of Software Engineering, Istanbul Ticaret University, 34445, Istanbul, Turkey

ARTICLE INFO

Keywords:
Generalized Klein–Gordon equation
Kink soliton
Jacobi elliptic functions
Nonlinear evolution equations
Traveling wave solutions

ABSTRACT

In this work, we investigate exact traveling wave solutions of higher-order generalized nonlinear Klein–Gordon equations using the ϕ^6-expansion method. Such nonlinear partial differential equations arise in various physical contexts, including fluid dynamics, nonlinear optics, and quantum field theory. The study focuses on obtaining analytical solutions for specific cases with nonlinearity indices $n = 1, 2, 3,$ and 5, corresponding to physically relevant scenarios. The solutions obtained are generated under specific constraint conditions derived from the parameter relationships and coefficient balance conditions that emerged during the application of the method. These constraints enable the fulfillment of reduced algebraic equations and guarantee the mathematical validity and physical applicability of the obtained wave solutions. Among these solutions, some solutions are expressed in terms of hyperbolic functions and exhibiting singularities at certain points represent wave structures that can be classified in the literature as singular hyperbolic traveling waves, trigonometric traveling waves, and singular periodic traveling wave solutions. Each solution is evaluated from a physical perspective, taking into account the relationships between the parameters in the model, and the behavior of the solution was examined for different values of the wave propagation parameter. The ϕ^6-method enables the derivation of compactons, solitons, solitary wave patterns, and periodic waveforms in a straightforward and efficient manner. Comparisons with previous solution techniques, such as the tanh-function method and the (G'/G)-expansion method, highlight the efficiency and elegance of the proposed approach. The results contribute to the broader understanding of nonlinear wave phenomena and provide analytical tools for further applications in theoretical and applied physics.

1. Introduction

The study of exact solutions to nonlinear partial differential equations (PDEs) has become increasingly vital in understanding complex physical phenomena, particularly in fields like fluid dynamics, plasma physics, and quantum mechanics. Among these, water wave models and nonlinear equations describing water waves have gained significant attention due to their relevance in both physics and mathematics. Nonlinear PDEs, which appear across many branches of natural science, describe a variety of wave phenomena, such as those found in shallow water, stratified flows, and hydrodynamics.

A central equation in the modeling of relativistic wave phenomena is the Klein-Gordon (KG) equation, which plays a pivotal role in understanding the dynamics of scalar fields and spin-zero particles. The KG equation is particularly influential in fields such as plasma physics, quantum field theory, internal waves, and hydrodynamics. Its Hamiltonian and Lagrangian structures enable integrability, leading to analytical solutions such as cnoidal waves and solitary waves, which provide crucial insights into wave phenomena in various media (Greiner and Müller, 1994; Greiner, 2000; Davydov, 1976; Sakurai, 1967; Weinberg, 2002). Historical Context of the Klein-Gordon Equation The Klein-Gordon equation was developed in 1926 by Oskar Klein and Walter Gordon, who sought to extend the Schrödinger equation, which describes non-relativistic particles, to relativistic particles (Gordon, 1926). This was motivated by the need to reconcile quantum mechanics with special relativity, particularly for particles that move at relativistic speeds. The equation arose from the relativistic energy-momentum relation, $E^2 = p^2c^2 + m^2c^4$, where E is the energy, p is the momentum, c is the speed of light, and m is the particle's mass. The resulting Klein-Gordon equation for a real scalar field $\phi(x,t)$ is given by:

$$\left(\frac{\partial^2}{\partial t^2} - c^2\nabla^2 + m^2c^4\right)\phi(x,t) = 0. \tag{1}$$

* Corresponding author.
E-mail addresses: asfyokus@yahoo.com (A. Yokus), maisah@ticaret.edu.tr (M.A. Isah), dogank@ticaret.edu.tr (D. Kaya).

https://doi.org/10.1016/j.oceaneng.2026.125239
Received 9 February 2026; Received in revised form 15 March 2026; Accepted 22 March 2026
Available online 31 March 2026
0029-8018/© 2026 Elsevier Ltd. All rights are reserved, including those for text and data mining, AI training, and similar technologies.

Although the equation provided a relativistic description of scalar particles, it also introduced a challenge: the appearance of negative energy solutions, which led to the development of the Dirac equation for spin-$\frac{1}{2}$ particles by Paul Dirac in 1928, addressing the issue of negative energy states (Feshbach and Villars, 1958).

Despite this, the Klein-Gordon equation remains an essential tool in quantum field theory and continues to play a crucial role in describing free scalar fields, including fields like the Higgs field in the Standard Model of particle physics. The equation is also foundational in cosmology, where it models scalar fields in inflationary models of the early universe (Weinberg, 2002).

In the broader context of nonlinear PDEs, solitonsöstable, localized wave-like solutions–often emerge. These solutions arise from the delicate balance between nonlinearity and dispersion in various systems. Solitons are prevalent in many physical phenomena, from fluid dynamics to optical fibers, and have been widely studied in the context of nonlinear SchrÃ¶dinger equations and soliton theory. Solitons are particularly useful in understanding complex wave interactions and have been applied in diverse fields such as telecommunications, cosmology, and nonlinear optics (Greiner, 2000).

Nonlinear evolution equations (NLEEs) are studied extensively across many fields of theoretical physics and applied mathematics, including biology and engineering. The investigation of exact NLEE solutions serves as a scientific method for clarifying these phenomena. Several successful approaches for obtaining accurate solutions to NLEEs have been introduced over the years. These include the new homoclinic test approach (Isah and Yokus, 2025; Yokus and Isah, 2023,?), the Bernoulli sub-equation method (Duran et al., 2021a), modified sub-equation method (Duran et al., 2021b), the modified $\frac{1}{G'}$-expansion technique (Yokus et al., 2025), the generalized exponential rational function approach (Ghanbari, 2019), the Jacobi elliptic function expansion method (Isah and Yokuş, 2026), the sine-Gordon expansion technique (Wazwaz, 2008), the Lie group approach (Iskenderoglu and Kaya, 2022), the modified Kudryashov technique (Ryabov et al., 2011), the modified extended tanh technique (Fan, 2000; Zaman et al., 2023), the modified simple equation approach (Kudryashov and Loguinova, 2008), improved Bernoulli sub-equation function method (Podder et al., 2025, 2023), the ϕ^6-model expansion method (Isah and Muhammad, 2025; Zayed and Al-Nowehy, 2020; Yokus and Isah, 2025), new auxiliary equation approach (Arefin et al., 2025), and the bilinear neural network approach (Isah et al., 2024b,a), among others. These methods have significantly contributed to the field of nonlinear partial differential equations over recent decades.

One of the most powerful tools for discovering N-soliton solutions for NLEEs is the Hirota method, discovered by Hirota in 1971. The Hirota method is advantageous because it simplifies the process of obtaining multi-soliton solutions without requiring complex mathematical computations. It has been successfully applied to various types of nonlinear PDEs, providing a way to transform the equations into new variables that make multi-soliton solutions appear in a particularly straightforward manner. Compared to other methods, such as inverse scattering transformation and various dressing techniques, the Hirota method stands out due to its algebraic nature rather than its analytic complexity (Hietarinta, 1987, 1997, 2005). The ability to generate multi-soliton solutions using the Hirota approach is particularly important because it allows soliton solutions for any equation that can be written in bilinear form.

The GK model has been widely used to mathematically represent shallow water waves on surfaces. Several approaches, including the inverse scattering transformation (Ablowitz et al., 1974), the bilinear method (Hietarinta, 1987), the Darboux transformation (Ali, 2018), and the novel ϕ^6-expansion approach (Zayed et al., 2018) are among the many strategies researchers have employed to obtain accurate solutions for the GK model. These approaches provide valuable insights into the nature of shallow water waves and contribute to the understanding of complex fluid dynamics in various settings.

The objective of this paper is to apply the ϕ^6-method to obtain exact traveling wave solutions of two classes of higher-order nonlinear equations such as the generalized nonlinear Klein–Gordon equation (Zhang and Ma, 1999; Li and Zhang, 2002; Kaya, 2005):

$$\eta_{tt} - k^2\eta_{xx} + a_1\eta - a_2\eta^{n+1} + a_3\eta^{2n+1} = 0 \tag{2}$$

with particular emphasis on the cases $n = 1, 2, 3,$ and 5, where $a_1, a_2, a_3,$ and k are real constants. Such equations are commonly used in mathematical physics to model nonlinear wave propagation. The η_{tt} term in the equation represents the second derivative of the wave field with respect to time, while the $k^2\eta_{xx}$ term expresses spatial propagation and dispersion effects. The $a_1\eta$ term represents the linear restoring term, while the $a_2\eta^{n+1}$ and $a_3\eta^{2n+1}$ terms represent high-order nonlinear contributions that characterize nonlinear interactions in the system. These nonlinear terms enable the model to describe different nonlinear regimes. Therefore, this equation provides a suitable mathematical framework for investigating complex wave behavior arising in various physical systems, such as nonlinear optics, field theory, and fluid dynamics. Eq. (2) plays a significant role in various scientific fields, including solid-state physics, nonlinear optics, and quantum field theory (see (Greiner and Müller, 1994; Greiner, 2000; Davydov, 1976; Sakurai, 1967; Weinberg, 2002)). Wazwaz (Wazwaz, 2005, 2006) investigated this class of nonlinear Klein–Gordon equations and discovered several types of exact traveling wave solutions, such as compactons, solitons, solitary wave patterns, and periodic waveforms, using the tanh-function method. Zayed and Gepreel (Zayed and Gepreel, 2011) successfully applied the $(\frac{G'}{G})$-expansion method to derive analytical solutions of Eq. (1). The novelty of the present work lies in the analytical investigation of a higher-order generalized nonlinear Klein–Gordon equation using the ϕ^6 expansion method. While several studies in the literature have applied different analytical techniques to classical nonlinear Klein–Gordon equations, the construction of exact traveling wave solutions for the considered generalized model remains limited. In this work, φ^6-six expansion framework is systematically employed to derive new classes of exact solutions under specific parametric constraint conditions arising from the coefficient balancing procedure. The obtained results reveal a variety of nonlinear wave structures, including singular hyperbolic traveling waves and singular periodic traveling waves expressed through hyperbolic and trigonometric functions. Moreover, the analysis is performed for different nonlinear indices $n = 1, 2, 3,$ and 5, allowing the model to capture different nonlinear regimes. This choice is not only due to mathematical convenience, but is also directly related to important model classes that arise in nonlinear field theory and wave dynamics. Nonlinear Klein–Gordon-type equations are widely used in scalar field theories to model self-interacting potentials. Models containing nonlinear terms of low order play a fundamental role in the study of topological solitons, kink solutions, and nonlinear wave structures. Higher nonlinear indices, on the other hand, represent stronger self-interactions within the field, enabling the investigation of more complex regimes of nonlinear wave dynamics. Therefore, the analysis of different nonlinear indices contributes to understanding both the mathematical structure and the physical behavior of the model over a wider parameter space. Such nonlinear Klein–Gordon models have been studied in detail in classical works on soliton theory and nonlinear wave propagation (Rajaraman, 1982). These findings extend existing analytical studies and provide additional exact solutions that may contribute to a deeper understanding of nonlinear wave propagation in generalized Klein–Gordon-type systems.

2. The φ^6-model expansion method

In this section, we provide a comprehensive description of the φ^6-model expansion method for deriving exact traveling wave solutions of nonlinear evolution equations. This method is particularly effective for obtaining a wide range of solutions, including solitons, singular soliton and periodic waveforms (Yokus and Isah, 2025).

Step 1: Assuming the nonlinear partial differential equation describing $\eta = (x,t)$ takes the following form:

$$Q(\eta, \eta_x, \eta_t, \eta_{xt}, \eta_{xx}, ...) = 0. \tag{3}$$

Here, Q is expressed as a polynomial function of $\eta(x,t)$, involving both the highest order partial derivatives and non-linear terms inherent in its formulation.

Step 2: Through the utilization of the wave transformation

$$\eta(x,t) = \eta(\mu), \quad \mu = x - ct. \tag{4}$$

In the scenario where c is indicative of the wave velocity, the Eq. (3) can be converted into below nonlinear ordinary differential equation.

$$\Omega(\eta, \eta', \eta\eta', \eta'', ...) = 0, \tag{5}$$

here the prime notation is used to indicate derivatives with respect to μ.

Step 3: Assuming the existence of a formal solution to Eq. (5):

$$\eta(\mu) = \sum_{j=0}^{2N} \delta_j \varphi^j(\mu). \tag{6}$$

To determine the degree of the polynomial expansion of the solution presented in Eq. (6), δ_j (for $j = 0, 1, 2, \ldots, N$) are constants to be established, the N value is calculated by balancing the highest-order linear term with the strongest nonlinear term (Yokus, 2011). This balancing procedure prevents the use of missing or unnecessary terms and ensures the mathematical consistency of the solution structure.

To implement this balancing procedure, we consider the homogeneous balance between η and its derivatives. If we denote the degree of $\eta(\mu)$ as $D[\eta] = N$ and the degree of $\frac{d^q\eta}{d\mu^q}$ as $D[\eta^{(q)}] = N + q$, then for a nonlinear term of the form $\eta^p\left(\frac{d^q\eta}{d\mu^q}\right)^s$, the degree is: $D\left[\eta^p\left(\frac{d^q\eta}{d\mu^q}\right)^s\right] = pN + s(N+q)$.

By equating the degrees of the highest-order derivative term and the dominant nonlinear term in Eq. (5), we obtain an algebraic equation for N, which is then solved to determine its value.

Step 4: $\varphi(\mu)$ adheres to the φ^6-model expansion in the following format:

$$\varphi'^2(\mu) = \tau_0 + \tau_2\varphi^2(\mu) + \tau_4\varphi^4(\mu) + \tau_6\varphi^6(\mu), \tag{7}$$
$$\varphi''(\mu) = \tau_2\varphi(\mu) + 2\tau_4\varphi^3(\mu) + 3\tau_6\varphi^5(\mu).$$

In this context, the constants τ_j (where $j = 0, 2, 4, 6$) are initially arbitrary and will be determined in subsequent stages.

Step 5: It is established that the solution to Eq. (7) takes the form:

$$\varphi(\mu) = \frac{Q(\mu)}{\sqrt{h_1 Q^2(\mu) + h_2}}. \tag{8}$$

$Q(\mu)$ denotes the solution to the Jacobi elliptic equation, ensuring the validity of $h_1 Q^2(\mu) + h_2 > 0$

$$Q'^2(\mu) = \mathcal{L}_0 + \mathcal{L}_2 Q^2(\mu) + \mathcal{L}_4 Q^4(\mu). \tag{9}$$

Here, the constants $\mathcal{L}_j$ (for $j = 0, 2, 4$) are unspecified and will be established through calculation. The values of h_2 and h_1 are provided by:

$$h_1 = \frac{\tau_4(\mathcal{L}_2 - \tau_2)}{(\mathcal{L}_2 - \tau_2)^2 + 3\mathcal{L}_0\mathcal{L}_4 - 2\mathcal{L}_2(\mathcal{L}_2 - \tau_2)}, \tag{10}$$
$$h_2 = \frac{3\mathcal{L}_0\tau_4}{(\mathcal{L}_2 - \tau_2)^2 + 3\mathcal{L}_0\mathcal{L}_4 - 2\mathcal{L}_2(\mathcal{L}_2 - \tau_2)}.$$

Subject to the specified condition

$$\tau_4^2(\mathcal{L}_2 - \tau_2)[9\mathcal{L}_0\mathcal{L}_4 - (\mathcal{L}_2 - \tau_2)(2\mathcal{L}_2 + \tau_2)] + 3\tau_6[-\mathcal{L}_2^2 + \tau_2^2 + 3\mathcal{L}_0\mathcal{L}_4]^2 = 0. \tag{11}$$

Step 5: The computation of Jacobi elliptic solutions for Eq. (9) is feasible under the condition with $0 < \alpha < 1$. Upon inserting Eq. (8) and Eq. (9) into Eq. (6), precise solutions for Eq. (3) can be derived.

Function	$\alpha \to 1$	$\alpha \to 0$	Function	$\alpha \to 1$	$\alpha \to 0$
$sn(\mu,\alpha)$	$tanh(\mu)$	$sin(\mu)$	$ds(\mu,\alpha)$	$csch(\mu)$	$csc(\mu)$
$cn(\mu,\alpha)$	$sech(\mu)$	$cos(\mu)$	$sc(\mu,\alpha)$	$sinh(\mu)$	$tan(\mu)$
$dn(\mu,\alpha)$	$sech(\mu)$	1	$sd(\mu,\alpha)$	$sinh(\mu)$	$sin(\mu)$
$ns(\mu,\alpha)$	$coth(\mu)$	$csc(\mu)$	$nc(\mu,\alpha)$	$cosh(\mu)$	$sec(\mu)$
$cs(\mu,\alpha)$	$csch(\mu)$	$cot(\mu)$	$cd(\mu,\alpha)$	1	$cos(\mu)$

3. Application of the φ^6-model expansion method to constructsolutions for the higher-order nonlinear Klein–Gordon equation

This section aims to review recent studies that apply the φ^6-model expansion method to the higher-order nonlinear Klein–Gordon equation, with a focus on deriving exact analytical solutions. The objective is to evaluate the method'ss efficiency, versatility, and advantages in handling complex nonlinear wave equations. The Klein–Gordon equation plays a fundamental role in modeling various physical phenomena, including dislocation dynamics in crystalline materials, relativistic quantum mechanics of elementary particles, and the propagation of fluxons in Josephson junctions.

$$\eta_{tt} - k^2\eta_{xx} + a_1\eta - a_2\eta^n + a_3\eta^{2n-1} = 0, \quad n > 2 \tag{12}$$

Consider the wave amplitude $\eta = \eta(x,t)$, where a_1, a_2 and a_3 are real constants. By introducing the traveling wave variable $\mu = x - ct$ and assuming a solution of the form $\eta(x,t) = \eta(\mu)$, Eqn (12) is transformed into an ordinary differential equation governing the behavior of η as a function of μ

$$\left(c^2 - k^2\right)\eta'' + a_1\eta - a_2\eta^n + a_3\eta^{2n-1} = 0. \tag{13}$$

The value $N = \frac{1}{n-1}$ is determined by applying the balancing principle between the highest-order derivative term η'' and the nonlinear term η^{2n-1}. Based on this result, we employ the following transformation:

$$\eta(\mu) = q^{\frac{1}{n-1}}(\mu). \tag{14}$$

By substituting Eq. (14) into Eq. (13) we get

$$\left(c^2 - k^2\right)\left[\frac{2-n}{(n-1)^2}(q')^2 + \frac{1}{(n-1)}qq''\right] + a_1q^2 - a_2q^3 + a_3q^4 = 0. \tag{15}$$

The balance parameter N is determined by analyzing the highest-order derivative term and the nonlinear term in Eq. (15), yielding $N = 1$. Based on this, the solution structure is accordingly constructed

$$q(\mu) = \delta_0 + \delta_1\varphi(\mu) + \delta_2\varphi^2(\mu). \tag{16}$$

The constants δ_0, δ_1, δ_2, δ_3, and δ_4 are unknown parameters to be determined through a systematic algebraic analysis in the following steps.

By substituting the assumed solution form given in Eq. (16) and the auxiliary equation in Eq. (7) into the reduced ordinary differential equation Eq. (15), and subsequently equating the coefficients of the polynomial terms $\varphi^j(\mu)$ for $j = 0$ to 8 to zero, a coupled system of nonlinear algebraic equations is obtained. This system governs the admissible parameter constraints and facilitates the determination of exact traveling wave solutions within the framework of the φ^6 -model expansion

method:

$$\begin{aligned}
&\varphi^0(\mu):\ a_3\delta_0^4-a_2\delta_0^3+a_1\delta_0^2+\frac{2\delta_2\delta_0c^2\tau_0}{n-1}+\frac{2\delta_1^2c^2\tau_0}{(n-1)^2}-\frac{\delta_1^2c^2\tau_0n}{(n-1)^2}-\frac{2\delta_2\delta_0\tau_0k^2}{n-1}\\
&+\frac{\delta_1^2\tau_0k^2n}{(n-1)^2}-\frac{2\delta_1^2\tau_0k^2}{(n-1)^2}=0,\\
&\varphi^1(\mu):\ 4a_3\delta_1\delta_0^3-3a_2\delta_1\delta_0^2+2a_1\delta_1\delta_0+\frac{\delta_1\delta_0c^2\tau_2}{n-1}+\frac{2\delta_1\delta_2c^2\tau_0}{n-1}\\
&+\frac{8\delta_1\delta_2c^2\tau_0}{(n-1)^2}-\frac{4\delta_1\delta_2c^2\tau_0n}{(n-1)^2}-\frac{\delta_1\delta_0\tau_2k^2}{n-1}+\frac{4\delta_1\delta_2\tau_0k^2n}{(n-1)^2}-\frac{2\delta_1\delta_2\tau_0k^2}{n-1}-\frac{8\delta_1\delta_2\tau_0k^2}{(n-1)^2}=0,\\
&\varphi^2(\mu):\ 4a_3\delta_2\delta_0^3+6a_3\delta_1^2\delta_0^2-3a_2\delta_2\delta_0^2-3a_2\delta_1^2\delta_0+2a_1\delta_2\delta_0+a_1\delta_1^2\\
&+\frac{4\delta_2\delta_0c^2\tau_2}{n-1}+\frac{\delta_1^2c^2\tau_2}{n-1}\\
&+\frac{2\delta_1^2c^2\tau_2}{(n-1)^2}+\frac{2\delta_2^2c^2\tau_0}{n-1}+\frac{8\delta_2^2c^2\tau_0}{(n-1)^2}-\frac{\delta_1^2c^2\tau_2n}{(n-1)^2}-\frac{4\delta_2^2c^2\tau_0n}{(n-1)^2}-\frac{4\delta_2\delta_0\tau_2k^2}{n-1}+\frac{\delta_1^2\tau_2k^2n}{(n-1)^2}\\
&+\frac{4\delta_2^2\tau_0k^2n}{(n-1)^2}-\frac{\delta_1^2\tau_2k^2}{n-1}-\frac{2\delta_2^2\tau_0k^2}{n-1}-\frac{2\delta_1^2\tau_2k^2}{(n-1)^2}-\frac{8\delta_2^2\tau_0k^2}{(n-1)^2}=0,\\
&\varphi^3(\mu):\ -a_2\delta_1^3+4a_3\delta_0\delta_1^3+12a_3\delta_0^2\delta_2\delta_1+2a_1\delta_2\delta_1-6a_2\delta_0\delta_2\delta_1\\
&+\frac{2\delta_0\delta_1c^2\tau_4}{n-1}+\frac{5\delta_2\delta_1c^2\tau_2}{n-1}\\
&+\frac{8\delta_2\delta_1c^2\tau_2}{(n-1)^2}-\frac{4\delta_2\delta_1c^2\tau_2n}{(n-1)^2}+\frac{4\delta_2\delta_1\tau_2k^2n}{(n-1)^2}-\frac{2\delta_0\delta_1\tau_4k^2}{n-1}-\frac{5\delta_2\delta_1\tau_2k^2}{n-1}-\frac{8\delta_2\delta_1\tau_2k^2}{(n-1)^2}=0,\\
&\varphi^4(\mu):\ a_3\delta_1^4-3a_2\delta_2\delta_1^2+12a_3\delta_0\delta_2\delta_1^2+6a_3\delta_0^2\delta_2^2+a_1\delta_2^2-3a_2\delta_0\delta_2^2\\
&+\frac{2\delta_1^2c^2\tau_4}{n-1}+\frac{2\delta_1^2c^2\tau_4}{(n-1)^2}-\frac{\delta_1^2c^2\tau_4n}{(n-1)^2}\\
&+\frac{4\delta_2^2c^2\tau_2}{n-1}+\frac{8\delta_2^2c^2\tau_2}{(n-1)^2}+\frac{6\delta_0\delta_2c^2\tau_4}{n-1}-\frac{4\delta_2^2c^2\tau_2n}{(n-1)^2}+\frac{\delta_1^2\tau_4k^2n}{(n-1)^2}-\frac{2\delta_1^2\tau_4k^2}{n-1}-\frac{2\delta_1^2\tau_4k^2}{(n-1)^2}\\
&+\frac{4\delta_2^2\tau_2k^2n}{(n-1)^2}-\frac{4\delta_2^2\tau_2k^2}{n-1}-\frac{6\delta_0\delta_2\tau_4k^2}{n-1}-\frac{8\delta_2^2\tau_2k^2}{(n-1)^2}=0,\\
&\varphi^5(\mu):\ 4a_3\delta_2\delta_1^3-3a_2\delta_2^2\delta_1+12a_3\delta_0\delta_2^2\delta_1+\frac{3\delta_0\delta_1c^2\tau_6}{n-1}+\frac{8\delta_2\delta_1c^2\tau_4}{n-1}+\frac{8\delta_2\delta_1c^2\tau_4}{(n-1)^2}\\
&-\frac{4\delta_2\delta_1c^2\tau_4n}{(n-1)^2}+\frac{4\delta_2\delta_1\tau_4k^2n}{(n-1)^2}-\frac{3\delta_0\delta_1\tau_6k^2}{n-1}-\frac{8\delta_2\delta_1\tau_4k^2}{n-1}-\frac{8\delta_2\delta_1\tau_4k^2}{(n-1)^2}=0,\\
&\varphi^6(\mu):\ -a_2\delta_2^3+4a_3\delta_0\delta_2^3+6a_3\delta_1^2\delta_2^2+\frac{6\delta_2^2c^2\tau_4}{n-1}+\frac{8\delta_2^2c^2\tau_4}{(n-1)^2}-\frac{4\delta_2^2c^2\tau_4n}{(n-1)^2}\\
&+\frac{8\delta_0\delta_2c^2\tau_6}{n-1}+\frac{3\delta_1^2c^2\tau_6}{n-1}+\frac{2\delta_1^2c^2\tau_6}{(n-1)^2}\\
&-\frac{\delta_1^2c^2\tau_6n}{(n-1)^2}+\frac{4\delta_2^2\tau_4k^2n}{(n-1)^2}-\frac{6\delta_2^2\tau_4k^2}{n-1}-\frac{8\delta_2^2\tau_4k^2}{(n-1)^2}-\frac{8\delta_0\delta_2\tau_6k^2}{n-1}+\frac{\delta_1^2\tau_6k^2n}{(n-1)^2}-\frac{3\delta_1^2\tau_6k^2}{n-1}\\
&-\frac{2\delta_1^2\tau_6k^2}{(n-1)^2}=0,\\
&\varphi^7(\mu):\ 4a_3\delta_1\delta_2^3+\frac{11\delta_1\delta_2c^2\tau_6}{n-1}+\frac{8\delta_1\delta_2c^2\tau_6}{(n-1)^2}-\frac{4\delta_1\delta_2c^2\tau_6n}{(n-1)^2}+\frac{4\delta_1\delta_2\tau_6k^2n}{(n-1)^2}\\
&-\frac{11\delta_1\delta_2\tau_6k^2}{n-1}-\frac{8\delta_1\delta_2\tau_6k^2}{(n-1)^2}=0,\\
&\varphi^8(\mu):\ a_3\delta_2^4+\frac{8\delta_2^2c^2\tau_6}{n-1}+\frac{8\delta_2^2c^2\tau_6}{(n-1)^2}-\frac{4\delta_2^2c^2\tau_6n}{(n-1)^2}+\frac{4\delta_2^2\tau_6k^2n}{(n-1)^2}-\frac{8\delta_2^2\tau_6k^2}{n-1}\\
&-\frac{8\delta_2^2\tau_6k^2}{(n-1)^2}=0.
\end{aligned}\tag{17}$$

The following solution is constructed by solving the algebraic system resulting from the method's consistency conditions

$$\delta_0=0,\quad \delta_1=0,\quad \tau_0=0,\quad \tau_4=\frac{a_2\delta_2(n-1)^2}{2(n+1)(c^2-k^2)},$$
$$\tau_6=-\frac{a_3\delta_2^2(n-1)^2}{4n(c^2-k^2)},\quad a_1=-\frac{4(c^2\tau_2-\tau_2k^2)}{(n-1)^2}.$$

By employing Eq. (8), (16), and (18) in conjunction with the Jacobi elliptic functions provided in the preceding table, exact analytical solutions to Eq. (12) are systematically derived.

1. When $\mathcal{L}_0=1$, $\mathcal{L}_2=-(1+\alpha^2)$, and $\mathcal{L}_4=\alpha^2$, with $0<\alpha<1$ are taken, the solution to the auxiliary equation yields the Jacobi elliptic function $Q(\mu)=sn(\mu,\alpha)$, which leads to the following traveling wave solution:

$$\eta_{1,0}(x,t)=\delta_2\left(\frac{sn(\mu,\alpha)}{\sqrt{h_1(sn(\mu,\alpha))^2+h_2}}\right)^2,\tag{18}$$

and if $\mathcal{L}_0=1$, $\mathcal{L}_2=-(1+\alpha^2)$, and $\mathcal{L}_4=\alpha^2$, with $0<\alpha<1$, the solution to the auxiliary equation yields the Jacobi elliptic function $Q(\mu)=cd(\mu,\alpha)$ then

$$\eta_{1,1}(x,t)=\delta_2\left(\frac{cd(\mu,\alpha)}{\sqrt{h_1(cd(\mu,\alpha))^2+h_2}}\right)^2.\tag{19}$$

Upon introducing the traveling wave transformation $\mu=x-ct$, the Jacobi elliptic functions $sn(\mu,\alpha)$ and $cd(\mu,\alpha)$, with elliptic modulus $0<\alpha<1$, exhibit degenerate behavior in the limits $\alpha\to0$ or $\alpha\to1$, reducing to periodic trigonometric or localized hyperbolic functions, respectively, as summarized in the preceding table. The corresponding expressions for h_1 and h_2, as defined in Eq. (10) are:

$$h_1=\frac{\tau_4(\tau_2+\alpha^2+1)}{-\tau_2^2+\alpha^4-\alpha^2+1},$$
$$h_2=-\frac{3\tau_4}{-\tau_2^2+\alpha^4-\alpha^2+1},$$

subject to the constraint condition

$$\tau_4^2(-\tau_2-\alpha^2-1)(-(-\tau_2+2\alpha^2-1)(\tau_2+\alpha^2-2))$$
$$+3\tau_6(\tau_2^2-\alpha^4+\alpha^2-1)^2=0.$$

By taking Eq. (18) into consideration, when $\alpha\to1$, then $sn(\mu,1)=\tanh(\mu)$, the kink soliton is retrieved (See fig. 1)

$$\eta_{1,2}(x,t)=\left(\frac{\delta_2\tanh^2(ct-x)}{\frac{a_2\delta_2(\tau_2+2)(n-1)^2\tanh^2(ct-x)}{2\left(1-\tau_2^2\right)(n+1)(c^2-k^2)}-\frac{3a_2\delta_2(n-1)^2}{2\left(1-\tau_2^2\right)(n+1)(c^2-k^2)}}\right)^{\frac{1}{n-1}},\tag{20}$$

where $\mu=x-ct$, such that

$$3\tau_6(\tau_2^2-1)^2+\tau_4^2(-\tau_2-2)((\tau_2-1)^2)=0.$$

As the modulus α tends to 0, the Jacobi elliptic function $sn(\mu,0)$ degenerates into $sin(\mu)$, yielding a periodic solution to the equation (See fig. 2)

$$\eta_{1,3}(x,t)=\left(\frac{\delta_2\sin^2(ct-x)}{\frac{3a_2\delta_2(n-1)^2}{2\left(\tau_2^2-1\right)(n+1)(c^2-k^2)}-\frac{a_2\delta_2(n-1)^2\sin^2(ct-x)}{2(\tau_2-1)(n+1)(c^2-k^2)}}\right)^{\frac{1}{n-1}},\tag{21}$$

such that

$$3\tau_6(\tau_2^2-1)^2+\tau_4^2(-\tau_2-1)(-(-\tau_2-1)(\tau_2-2))=0.$$

By examining the behavior of the Jacobi elliptic function $cd(\mu,\alpha)$ in the limits $\alpha\to1$ (where $cd(\mu,1)=1$) and $\alpha\to0$ (where $cd(\mu,0)=\cos(\mu)$) in Eq. (19), different classes of solutions ranging from constant amplitude waves to periodic structures can be obtained.

2. When $\mathcal{L}_0=1-\alpha^2$, $\mathcal{L}_2=2\alpha^2-1$, and $\mathcal{L}_4=-\alpha^2$, with $0<\alpha<1$, the solution to the auxiliary equation yields the Jacobi elliptic function $Q(\mu)=cn(\mu,\alpha)$, which leads to the following traveling wave solution:

$$\eta_{2,1}(x,t)=\delta_2\left(\frac{cn(\mu,\alpha)}{\sqrt{h_1(cn(\mu,\alpha))^2+h_2}}\right)^2,\tag{22}$$

where the values of h_1 and h_2 are ascertained by

$$h_1=\frac{\tau_4(\tau_2-2\alpha^2+1)}{-\tau_2^2+\alpha^4-\alpha^2+1},$$
$$h_2=\frac{3\tau_4(\alpha^2-1)}{-\tau_2^2+\alpha^4-\alpha^2+1},$$

under the specified constraint $3\tau_6\left(\tau_2^2-3\left(1-\alpha^2\right)\alpha^2-\left(2\alpha^2-1\right)^2\right)^2+\tau_4^2(-\tau_2+2\alpha^2-1)(-(-\tau_2+2\alpha^2-1)(\tau_2+2(2\alpha^2-1))-9(1-\alpha^2)\alpha^2)=0$.

If $\alpha\to1$, $cn(\mu,1)=sech(\mu)$ then the trivial solution is retrieved, provided that

$$3\tau_6\left(\tau_2^2-1\right)^2+\tau_4^2(1-\tau_2)(-(1-\tau_2)(\tau_2+2))=0.$$

As α approaches 0, the solution becomes periodic (See fig. 3)

$$\eta_{2,2}(x,t)=\left(\frac{\delta_2\cos^2(ct-x)}{\frac{3a_2\delta_2(n-1)^2}{2\left(\tau_2^2-1\right)(n+1)(c^2-k^2)}-\frac{a_2\delta_2(n-1)^2\cos^2(ct-x)}{2(\tau_2-1)(n+1)(c^2-k^2)}}\right)^{\frac{1}{n-1}},\tag{23}$$

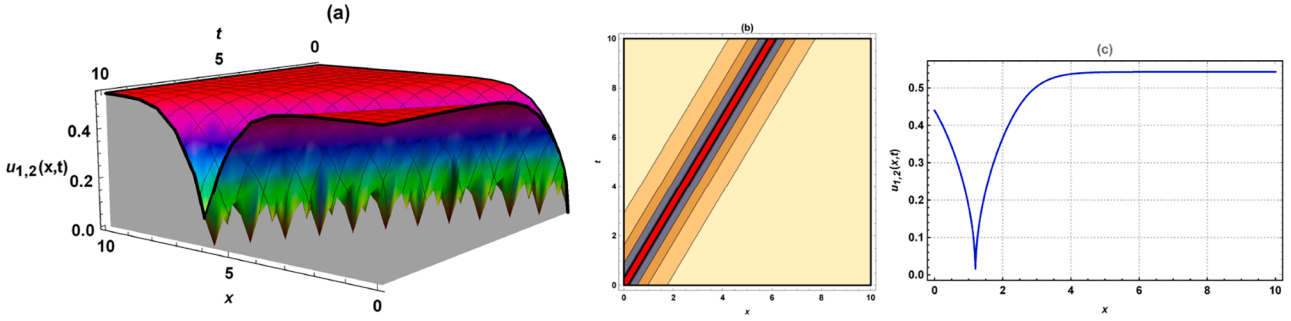


Fig. 1. The visual depiction of the solution provided in Eq. (20), particularly as α approaches 1, (a) is the 3D graphic, (b) is the contour graphic while (c) is the 2D graphic for $c = 0.6,\ n = 5,\ \delta_2 = 0.4,\ k = 0.55,\ a_2 = -0.5,\ \tau_2 = 0.01$..

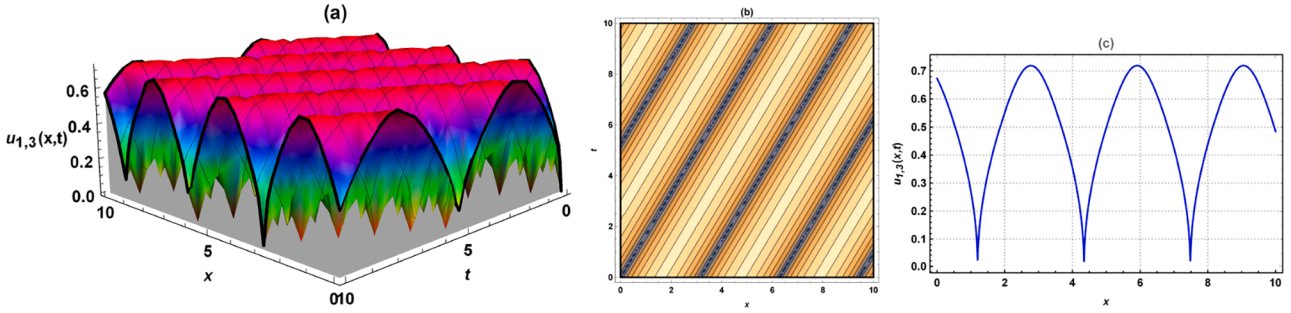


Fig. 2. Visual representation of the solution $\eta_{1,3}(x,t)$ given by Eq. (21) in the limit as $\alpha \to 0$. (a) Three-dimensional profile showing wave propagation, (b) two-dimensional contour plot illustrating the wavefronts, and (c) Two-dimensional view at fixed time, highlighting the oscillatory structure. The parameters are set as $c = 0.6,\ n = 5,\ \delta_2 = 0.4,\ k = 0.05,\ a_2 = -0.5,\ \tau_2 = 0.5$..

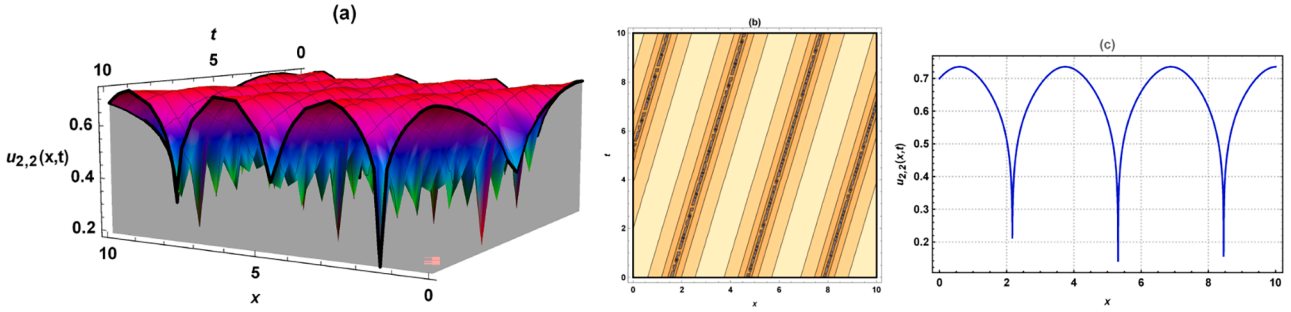


Fig. 3. Visual representation of the solution $\eta_{2,2}(x,t)$ given by Eq. (23) in the limit as $\alpha \to 0$. (a) Three-dimensional profile showing wave propagation, (b) two-dimensional contour plot illustrating the wavefronts, and (c) Two-dimensional view at fixed time, highlighting the oscillatory structure. The parameters are set as $c = 0.3,\ n = 12,\ \delta_2 = 0.1,\ k = 0.8,\ a_2 = 1.8,\ \tau_2 = 0.1$..

such that

$$3\tau_6\left(\tau_2^2-1\right)^2+\tau_4^2\left(-\tau_2-1\right)\left(-\left(-\tau_2-1\right)\left(\tau_2-2\right)\right)=0.$$

3. If $\mathcal{L}_0 = \alpha^2 - 1$, $\mathcal{L}_2 = 2 - \alpha^2$, and $\mathcal{L}_4 = -1$, with $0 < \alpha < 1$, the solution to the auxiliary equation yields the Jacobi elliptic function $Q(\mu) = dn(\mu, \alpha)$ which results

$$\eta_{3,1}(x,t)=\delta_2\left(\frac{dn(\mu,\alpha)}{\sqrt{h_1(dn(\mu,\alpha))^2+h_2}}\right)^2, \tag{24}$$

where the values of h_1 and h_2 are ascertained by

$$h_1=\frac{\tau_4\left(\tau_2+\alpha^2-2\right)}{-\tau_2^2+\alpha^4-\alpha^2+1},$$
$$h_2=-\frac{3\tau_4\left(\alpha^2-1\right)}{-\tau_2^2+\alpha^4-\alpha^2+1},$$

subject to the constraint condition $\tau_4^2\left(-\tau_2-\alpha^2+2\right)\left(-\left(-\tau_2-\alpha^2+2\right)\left(\tau_2+2\left(2-\alpha^2\right)\right)-9\left(\alpha^2-1\right)\right)+3\tau_6\left(\tau_2^2-\left(2-\alpha^2\right)^2-3\left(\alpha^2-1\right)\right)^2=0.$

If $\alpha \to 1$, then the rational solution is obtained, provided that

$$3\tau_6\left(\tau_2^2-1\right)^2+\tau_4^2\left(1-\tau_2\right)\left(-\left(1-\tau_2\right)\left(\tau_2+2\right)\right)=0.$$

If $\alpha \to 0$, then the rational solution is obtained, such that

$$3\tau_6\left(\tau_2^2-1\right)^2+\tau_4^2\left(2-\tau_2\right)\left(9-\left(2-\tau_2\right)\left(\tau_2+4\right)\right)=0.$$

4. If $\mathcal{L}_0 = \alpha^2$, $\mathcal{L}_2 = -\left(1+\alpha^2\right)$, and $\mathcal{L}_4 = 1$, with $0 < \alpha < 1$, then the solution to the auxiliary equation yields the Jacobi elliptic function $Q(\mu) = ns(\mu, \alpha)$ or $Q(\mu) = dc(\mu, \alpha)$ which results

$$\eta_{4,0}(x,t)=\delta_2\left(\frac{ns(\mu,\alpha)}{\sqrt{h_1(ns(\mu,\alpha))^2+g}}\right)^2, \tag{25}$$

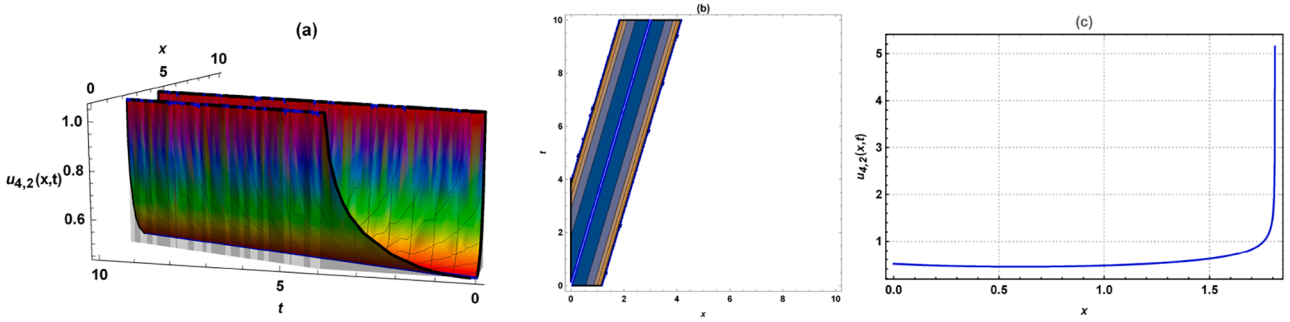


Fig. 4. Visual representation of the solution $\eta_{4,2}(x,t)$ given by Eq. (27) in the limit as $\alpha \to 1$. (a) Three-dimensional profile showing wave propagation, (b) two-dimensional contour plot illustrating the wavefronts, and (c) Two-dimensional view at fixed time, highlighting the oscillatory structure. The parameters are set as $c = 0.3,\ n = 5,\ \delta_2 = 0.1,\ k = 0.002,\ a_2 = 0.8,\ \tau_2 = 0.1$..

or

$$\eta_{4,1}(x,t) = \delta_2\left(\frac{dc(\mu,\alpha)}{\sqrt{h_1(dc(\mu,\alpha))^2 + h_2}}\right)^2, \tag{26}$$

where the values of h_1 and h_2 are ascertained by

$$h_1 = \frac{\tau_4\left(\tau_2 + \alpha^2 + 1\right)}{-\tau_2^2 + \alpha^4 - \alpha^2 + 1},$$
$$h_2 = -\frac{3\tau_4\alpha^2}{-\tau_2^2 + \alpha^4 - \alpha^2 + 1},$$

under the constraint condition

$$3\tau_6\left(\tau_2^2 - 1\right)^2 + \tau_4^2(-\tau_2 - 2)\left(9 - (-\tau_2 - 2)(\tau_2 - 4)\right) = 0.$$

If $\alpha \to 1$, then the soliton solution is obtained (See fig. 4)

$$\eta_{4,2}(x,t) = \left(\frac{\delta_2 \coth^2(ct - x)}{\frac{3a_2\delta_2(n-1)^2}{2\left(\tau_2^2-1\right)(n+1)(c^2-k^2)} - \frac{a_2\delta_2(\tau_2+2)(n-1)^2\coth^2(ct-x)}{2\left(\tau_2^2-1\right)(n+1)(c^2-k^2)}}\right)^{\frac{1}{n-1}}, \tag{27}$$

such that

$$3\tau_6\left(\tau_2^2 - 1\right)^2 + \tau_4^2(-\tau_2 - 2)\left(9 - (-\tau_2 - 2)(\tau_2 - 4)\right) = 0.$$

If $\alpha \to 0$, then the rational solution is obtained, such that

$$3\tau_6\left(\tau_2^2 - 1\right)^2 + \tau_4^2(-\tau_2 - 1)\left(-(-\tau_2 - 1)(\tau_2 - 2)\right) = 0.$$

5. Assuming $\mathcal{L}_0 = -\alpha^2$, $\mathcal{L}_2 = 2\alpha^2 - 1$, and $\mathcal{L}_4 = 1 - \alpha^2$, with $0 < \alpha < 1$, the solution to the auxiliary equation yields the Jacobi elliptic function $Q(\mu) = nc(\mu,\alpha)$, resulting to:

$$\eta_{5,1}(x,t) = \delta_2\left(\frac{nc(\mu,\alpha)}{\sqrt{h_1(nc(\mu,\alpha))^2 + h_2}}\right)^2, \tag{28}$$

where the values of h_1 and h_2 are ascertained by

$$h_1 = \frac{\tau_4\left(\tau_2 - 2\alpha^2 + 1\right)}{-\tau_2^2 + \alpha^4 - \alpha^2 + 1},$$
$$h_2 = \frac{3\tau_4\alpha^2}{-\tau_2^2 + \alpha^4 - \alpha^2 + 1},$$

under the constraint condition

$$3\tau_6\left(\tau_2^2 - 1\right)^2 + \tau_4^2(1 - \tau_2)\left(-(1 - \tau_2)(\tau_2 + 2)\right) = 0.$$

If $\alpha \to 1$, then the dark-type soliton solution is obtained (See fig. 5)

$$\eta_{5,2}(x,t) = \left(\frac{\delta_2 \cosh^2(ct - x)}{\frac{3a_2\delta_2(n-1)^2}{2\left(1-\tau_2^2\right)(n+1)(c^2-k^2)} - \frac{a_2\delta_2(1-\tau_2)(n-1)^2\cosh^2(ct-x)}{2\left(1-\tau_2^2\right)(n+1)(c^2-k^2)}}\right)^{\frac{1}{n-1}}, \tag{29}$$

such that

$$3\tau_6\left(\tau_2^2 - 1\right)^2 + \tau_4^2(1 - \tau_2)\left(-(1 - \tau_2)(\tau_2 + 2)\right) = 0.$$

If $\alpha \to 0$, then the rational solution is obtained, such that

$$3\tau_6\left(\tau_2^2 - 1\right)^2 + \tau_4^2(-\tau_2 - 1)\left(-(-\tau_2 - 1)(\tau_2 - 2)\right) = 0.$$

6. Assuming $\mathcal{L}_0 = -1$, $\mathcal{L}_2 = 2 - \alpha^2$, and $\mathcal{L}_4 = -(1 - \alpha^2)$, with $0 < \alpha < 1$, the solution to the auxiliary equation yields the Jacobi elliptic function $Q(\mu) = nd(\mu,\alpha)$, which leads to the following traveling wave solution:

$$\eta_{6,1}(x,t) = \delta_2\left(\frac{nd(\mu,\alpha)}{\sqrt{h_1(nd(\mu,\alpha))^2 + h_2}}\right)^2, \tag{30}$$

where the values of h_1 and h_2 are ascertained by

$$h_1 = \frac{\tau_4\left(\tau_2 + \alpha^2 - 2\right)}{-\tau_2^2 + \alpha^4 - \alpha^2 + 1},$$
$$h_2 = \frac{3\tau_4}{-\tau_2^2 + \alpha^4 - \alpha^2 + 1},$$

subject to the specified condition $3\tau_6\left(\tau_2^2 - \left(2 - \alpha^2\right)^2 - 3\left(\alpha^2 - 1\right)\right)^2 + \tau_4^2(-\tau_2 - \alpha^2 + 2)\left(-(-\tau_2 - \alpha^2 + 2)\left(\tau_2 + 2\left(2 - \alpha^2\right)\right) - 9\left(\alpha^2 - 1\right)\right) = 0$.

In the limit as $\alpha \to 1$, the Jacobi elliptic function degenerates into a hyperbolic form, leading to the emergence of a singular soliton solution (See fig. 6)

$$\eta_{6,2}(x,t) = \left(\frac{\delta_2 \cosh^2(ct - x)}{-\frac{3a_2\delta_2(n-1)^2}{2\left(\tau_2^2-1\right)(n+1)(c^2-k^2)} - \frac{a_2\delta_2(n-1)^2\cosh^2(ct-x)}{2(\tau_2+1)(n+1)(c^2-k^2)}}\right)^{\frac{1}{n-1}}, \tag{31}$$

such that

$$3\tau_6\left(\tau_2^2 - 1\right)^2 + \tau_4^2(1 - \tau_2)\left(-(1 - \tau_2)(\tau_2 + 2)\right) = 0.$$

7. If $\mathcal{L}_0 = 1$, $\mathcal{L}_2 = 2 - \alpha^2$, $\mathcal{L}_4 = 1 - \alpha^2$, $0 < \alpha < 1$, then $Q(\mu) = sc(\mu,\alpha)$, resulting in

$$\eta_{7,1}(x,t) = \delta_2\left(\frac{sc(\mu,\alpha)}{\sqrt{h_1(sc(\mu,\alpha))^2 + h_2}}\right)^2, \tag{32}$$

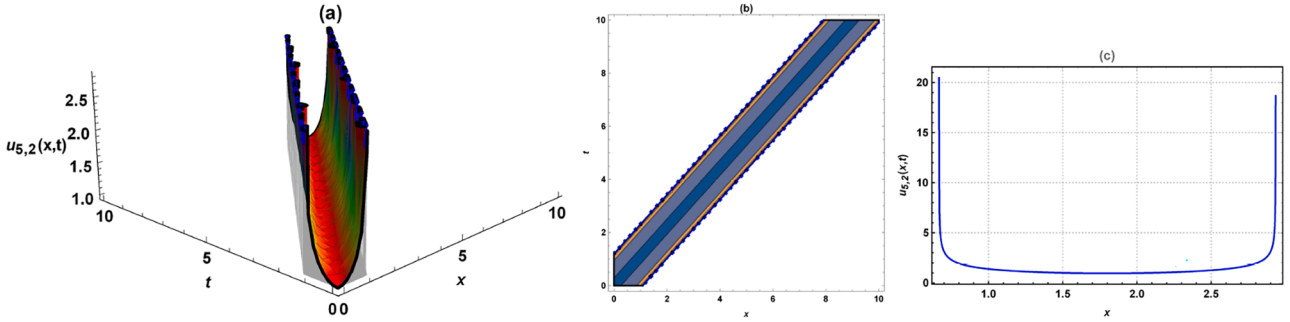


Fig. 5. Visual representation of the solution $\eta_{5,2}(x,t)$ given by Eq. (29) in the limit as $\alpha \to 1$. (a) Three-dimensional profile showing wave propagation, (b) two-dimensional contour plot illustrating the wavefronts, and (c) Two-dimensional view at fixed time, highlighting the oscillatory structure. The simulation is performed with the parameter values $c = 0.9,\ n = 4,\ k = 0.1,\ a_2 = 0.5,\ \tau_2 = -0.02$..

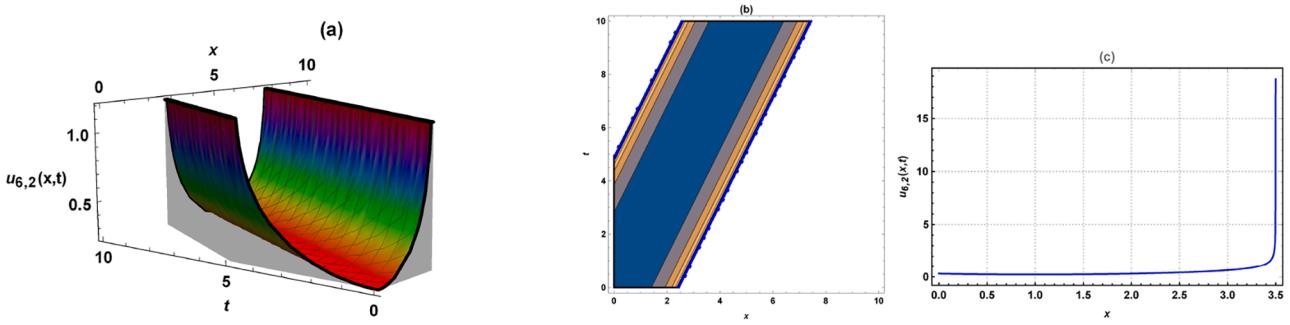


Fig. 6. Visual representation of the solution $\eta_{6,2}(x,t)$ given by Eq. (31) in the limit as $\alpha \to 1$. (a) Three-dimensional profile showing wave propagation, (b) contour plot illustrating the wavefronts, and (c) 2D view at fixed time, highlighting the oscillatory structure. The simulation is performed with the parameter values $c = 0.5,\ n = 4,\ k = 0.2,\ a_2 = 1.01,\ \tau_2 = -0.92$..

where the values of h_1 and h_2 are ascertained by

$$h_1 = \frac{\tau_4\left(\tau_2 + \alpha^2 - 2\right)}{-\tau_2^2 + \alpha^4 - \alpha^2 + 1},$$
$$h_2 = -\frac{3\tau_4}{-\tau_2^2 + \alpha^4 - \alpha^2 + 1},$$

subject to the specified condition $3\tau_6\left(\tau_2^2 - \left(2 - m^2\right)^2 + 3\left(1 - m^2\right)\right)^2 + \tau_4^2\left(-\tau_2 - m^2 + 2\right)\left(9\left(1 - m^2\right) - \left(-\tau_2 - m^2 + 2\right)\left(\tau_2 + 2\left(2 - m^2\right)\right)\right) = 0$.

If $\alpha \to 1$, then the soliton solution is obtained (See fig. 7)

$$\eta_{7,2}(x,t) = \left(\frac{\delta_2 \sinh^2(ct - x)}{\frac{3a_2\delta_2(n-1)^2}{2\left(\tau_2^2-1\right)(n+1)\left(c^2-k^2\right)} - \frac{a_2\delta_2(n-1)^2 \sinh^2(ct-x)}{2\left(\tau_2+1\right)(n+1)\left(c^2-k^2\right)}}\right)^{\frac{1}{n-1}}, \tag{33}$$

such that

$$3\tau_6\left(\tau_2^2 - 1\right)^2 + \tau_4^2\left(1 - \tau_2\right)\left(-\left(1 - \tau_2\right)\left(\tau_2 + 2\right)\right) = 0.$$

As α tends to 0, the solution becomes a periodic wave (See fig. 8)

$$\eta_{7,3}(x,t) = \left(\frac{\delta_2 \tan^2(ct - x)}{\frac{3a_2\delta_2(n-1)^2}{2\left(\tau_2^2-1\right)(n+1)\left(c^2-k^2\right)} - \frac{a_2\delta_2\left(\tau_2-2\right)(n-1)^2 \tan^2(ct-x)}{2\left(\tau_2^2-1\right)(n+1)\left(c^2-k^2\right)}}\right)^{\frac{1}{n-1}}, \tag{34}$$

such that

$$3\tau_6\left(\tau_2^2 - 1\right)^2 + \tau_4^2\left(2 - \tau_2\right)\left(9 - \left(2 - \tau_2\right)\left(\tau_2 + 4\right)\right) = 0.$$

8. If $\mathcal{L}_0 = 1,\ \mathcal{L}_2 = 2\alpha^2 - 1,\ \mathcal{L}_4 = -\alpha^2\left(1 - \alpha^2\right),\ 0 < \alpha < 1,$ then $Q(\mu) = sd(\mu,\alpha)$ resulting in

$$\eta_{8,1}(x,t) = \delta_2\left(\frac{sd(\mu,\alpha)}{\sqrt{h_1(sd(\mu,\alpha))^2 + h_2}}\right)^2, \tag{35}$$

where the values of h_1 and h_2 are ascertained by

$$h_1 = \frac{\tau_4\left(\tau_2 - 2\alpha^2 + 1\right)}{-\tau_2^2 + \alpha^4 - \alpha^2 + 1},$$
$$h_2 = -\frac{3\tau_4}{-\tau_2^2 + \alpha^4 - \alpha^2 + 1},$$

under the constraint condition $3\tau_6\left(\tau_2^2 - 3\left(1 - \alpha^2\right)\alpha^2 - \left(2\alpha^2 - 1\right)^2\right)^2 + \tau_4^2\left(-\tau_2 + 2\alpha^2 - 1\right)\left(-\left(-\tau_2 + 2\alpha^2 - 1\right)\left(\tau_2 + 2\left(2\alpha^2 - 1\right)\right) - 9\left(1 - \alpha^2\right)\alpha^2\right) = 0$.

If $\alpha \to 1$, then the dark-type soliton solution is obtained (See fig. 9)

$$\eta_{8,2}(x,t) = \left(\frac{\delta_2 \sinh^2(ct - x)}{\frac{3a_2\delta_2(n-1)^2}{2\left(\tau_2^2-1\right)(n+1)\left(c^2-k^2\right)} - \frac{a_2\delta_2(n-1)^2 \sinh^2(ct-x)}{2\left(\tau_2+1\right)(n+1)\left(c^2-k^2\right)}}\right)^{\frac{1}{n-1}}, \tag{36}$$

such that

$$3\tau_6\left(\tau_2^2 - 1\right)^2 + \tau_4^2\left(1 - \tau_2\right)\left(-\left(1 - \tau_2\right)\left(\tau_2 + 2\right)\right) = 0.$$

9. If $\mathcal{L}_0 = 1 - \alpha^2,\ \mathcal{L}_2 = 2 - \alpha^2$, and $\mathcal{L}_4 = 1$, with $0 < \alpha < 1$, then the solution to the auxiliary equation yields the Jacobi elliptic function $Q(\mu) = cs(\mu,\alpha)$ then

$$\eta_{9,1}(x,t) = \delta_2\left(\frac{cs(\mu,\alpha)}{\sqrt{h_1(cs(\mu,\alpha))^2 + h_2}}\right)^2, \tag{37}$$

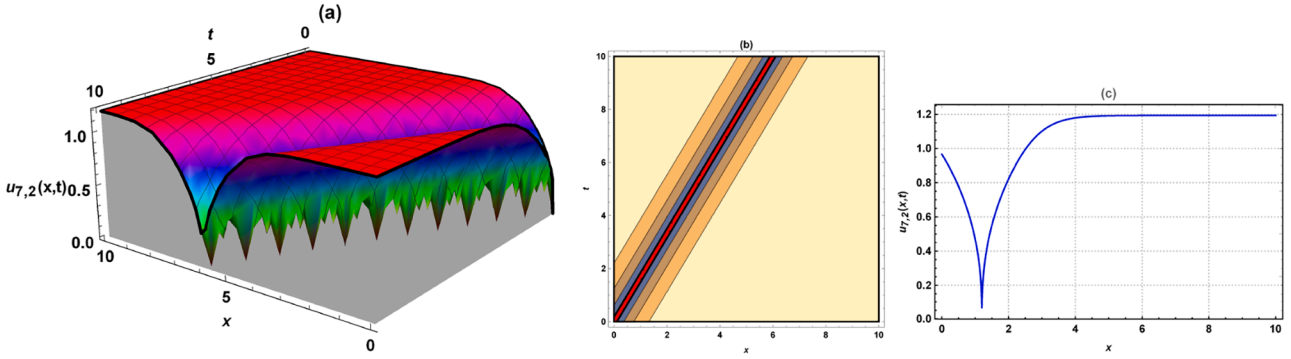


Fig. 7. Visual representation of the solution $\eta_{7,2}(x,t)$ given by Eq. (33) in the limit as $\alpha \to 1$. (a) Three-dimensional profile showing wave propagation, (b) contour plot illustrating the wavefronts, and (c) 2D view at fixed time, highlighting the oscillatory structure. The simulation is performed with the parameter values $c = 0.6,\ n = 6,\ k = 1.3,\ a_2 = 0.4,\ \tau_2 = 0.3$..

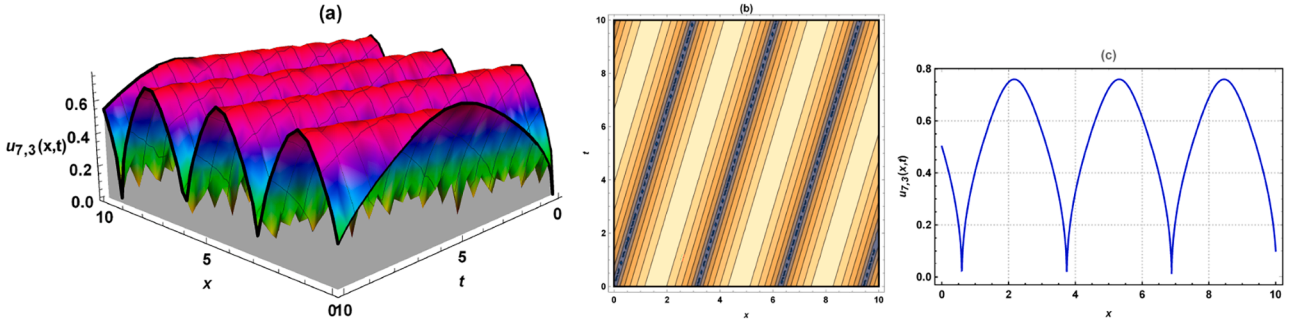


Fig. 8. Visual representation of the solution $\eta_{7,3}(x,t)$ given by Eq. (34) in the limit as $\alpha \to 0$. (a) Three-dimensional profile showing wave propagation, (b) contour plot illustrating the wavefronts, and (c) 2D view at fixed time, highlighting the oscillatory structure. The simulation is performed with the parameter values $c = 0.3,\ n = 5,\ k = 1.3,\ a_2 = 1.8,\ \tau_2 = 0.5$..

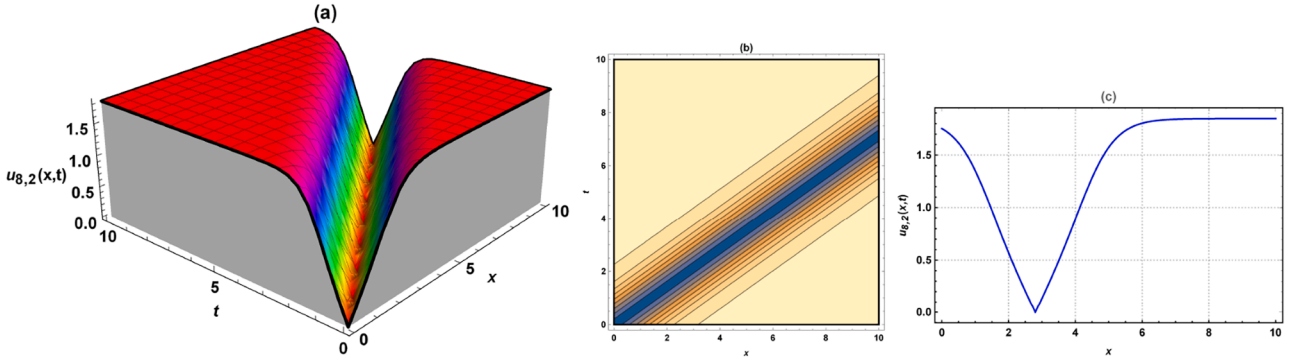


Fig. 9. Visual representation of the solution $\eta_{8,2}(x,t)$ given by Eq. (36) in the limit as $\alpha \to 1$. (a) Three-dimensional profile showing wave propagation, (b) contour plot illustrating the wavefronts, and (c) 2D view at fixed time, highlighting the oscillatory structure. The simulation is performed with the parameter values $c = 1.4,\ n = 3,\ k = 0.2,\ a_2 = -1.8,\ \tau_2 = 0.6$..

where the values of h_1 and h_2 are ascertained by

$$h_1 = \frac{\tau_4(\tau_2 + \alpha^2 - 2)}{-\tau_2^2 + \alpha^4 - \alpha^2 + 1},$$
$$h_2 = \frac{3\tau_4(\alpha^2 - 1)}{-\tau_2^2 + \alpha^4 - \alpha^2 + 1},$$

under the constraint condition $3\tau_6\left(\tau_2^2 - \left(2-\alpha^2\right)^2 + 3\left(1-\alpha^2\right)\right)^2 + \tau_4^2\left(-\tau_2 - \alpha^2 + 2\right)\left(9\left(1-\alpha^2\right) - \left(-\tau_2 - \alpha^2 + 2\right)\left(\tau_2 + 2\left(2-\alpha^2\right)\right)\right) = 0$.

If $\alpha \to 1$, then the rational solution is obtained, such that

$$3\tau_6\left(\tau_2^2 - 1\right)^2 + \tau_4^2\left(1-\tau_2\right)\left(-\left(1-\tau_2\right)\left(\tau_2 + 2\right)\right) = 0.$$

In the limit as $\alpha \to 0$, the Jacobi elliptic function degenerates into a hyperbolic form, leading to the emergence of a periodic wave (See fig. 10)

$$\eta_{9,3}(x,t) = \left(\frac{\delta_2 \cot^2(ct - x)}{\frac{3a_2\delta_2(n-1)^2}{2\left(\tau_2^2-1\right)(n+1)\left(c^2-k^2\right)} - \frac{a_2\delta_2(\tau_2-2)(n-1)^2\cot^2(ct-x)}{2\left(\tau_2^2-1\right)(n+1)\left(c^2-k^2\right)}} \right)^{\frac{1}{n-1}}, \tag{38}$$

such that

$$3\tau_6\left(\tau_2^2 - 1\right)^2 + \tau_4^2\left(2-\tau_2\right)\left(9 - \left(2-\tau_2\right)\left(\tau_2 + 4\right)\right) = 0.$$

10. If $\mathcal{L}_0 = -\alpha^2\left(1-\alpha^2\right)$, $\mathcal{L}_2 = 2\alpha^2 - 1$, and $\mathcal{L}_4 = 1$, with $0 < \alpha < 1$, then then the solution to the auxiliary equation yields the Jacobi elliptic

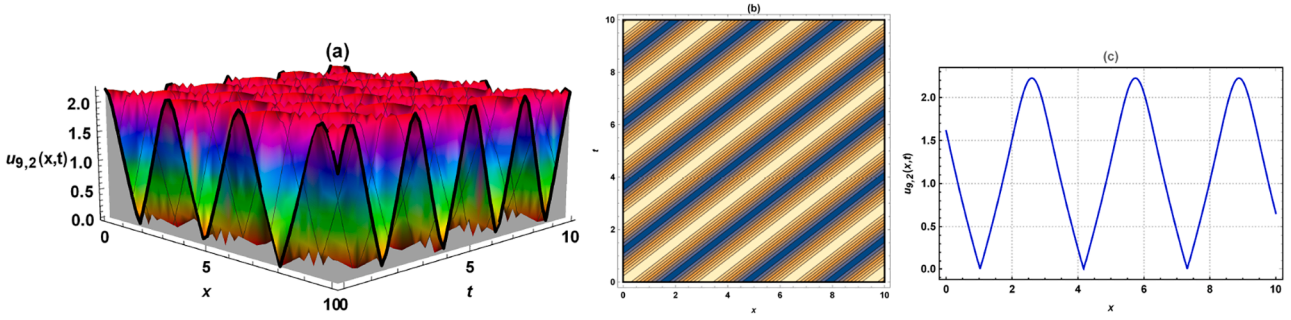


Fig. 10. Visual representation of the solution $\eta_{9,3}(x,t)$ given by Eq. (38) in the limit as $\alpha \to 0$. (a) Three-dimensional profile showing wave propagation, (b) contour plot illustrating the wavefronts, and (c) 2D view at fixed time, highlighting the oscillatory structure. The simulation is performed with the parameter values $c = 1.3,\ n = 3,\ k = 0.2,\ a_2 = -0.2,\ \tau_2 = 0.8$..

function $Q(\mu) = ds(\mu,\alpha)$, we have

$$\eta_{10}(x,t) = \delta_2\left(\frac{ds(\mu,\alpha)}{\sqrt{h_1(ds(\mu,\alpha))^2 + h_2}}\right)^2, \tag{39}$$

where the values of h_1 and h_2 are ascertained by

$$h_1 = \frac{\tau_4\left(\tau_2 - 2\alpha^2 + 1\right)}{-\tau_2^2 + \alpha^4 - \alpha^2 + 1},$$
$$h_2 = -\frac{3\tau_4\alpha^2\left(\alpha^2 - 1\right)}{-\tau_2^2 + \alpha^4 - \alpha^2 + 1},$$

under the constraint condition $3\tau_6\left(\tau_2^2 - 3\left(1-\alpha^2\right)\alpha^2 - \left(2\alpha^2-1\right)^2\right)^2 + \tau_4^2\left(-\tau_2 + 2\alpha^2 - 1\right)\left(-\left(-\tau_2 + 2\alpha^2 - 1\right)\left(\tau_2 + 2\left(2\alpha^2-1\right)\right) - 9\left(1-\alpha^2\right)\alpha^2\right) = 0$.

11. If $\mathcal{L}_0 = \frac{1-\alpha^2}{4}$, $\mathcal{L}_2 = \frac{1+\alpha^2}{2}$, $\mathcal{L}_4 = \frac{1-\alpha^2}{4}$, $0 < \alpha < 1$, then $Q(\mu) = nc(\mu,\alpha) \pm sc(\mu,\alpha)$ or $Q(\mu) = \frac{cn(\mu,\alpha)}{1\pm sn(\mu,\alpha)}$, we have

$$\eta_{11,0}(x,t) = \delta_2\left(\frac{nc(\mu,\alpha) \pm sc(\mu,\alpha)}{\sqrt{h_1(nc(\mu,\alpha) \pm sc(\mu,\alpha))^2 + h_2}}\right)^2, \tag{40}$$

or

$$\eta_{11,1}(x,t) = \delta_2\left(\frac{\frac{cn(\mu,\alpha)}{1\pm sn(\mu,\alpha)}}{\sqrt{h_1\left(\frac{cn(\mu,\alpha)}{1\pm sn(\mu,\alpha)}\right)^2 + h_2}}\right)^2, \tag{41}$$

where the values of h_1 and h_2 are ascertained by

$$h_1 = -\frac{8\tau_4\left(-2\tau_2 + \alpha^2 + 1\right)}{-16\tau_2^2 + \alpha^4 + 14\alpha^2 + 1},$$
$$h_2 = \frac{12\tau_4\left(\alpha^2 - 1\right)}{-16\tau_2^2 + \alpha^4 + 14\alpha^2 + 1},$$

under the constraint condition $3\tau_6\left(\tau_2^2 + \frac{3}{16}\left(1-m^2\right)^2 - \frac{1}{4}\left(m^2+1\right)^2\right)^2 + \tau_4^2\left(\frac{1}{2}\left(m^2+1\right) - \tau_2\right)\left(\frac{9}{16}\left(1-m^2\right)^2 - \left(\frac{1}{2}\left(m^2+1\right) - \tau_2\right)\left(\tau_2 + m^2 + 1\right)\right) = 0$.

As α tends toward 0, the solution becomes combined periodic waves (See Figs. 11 and 12)

$$\eta_{11,2}(x,t) = \left(\frac{\delta_2(\sec(ct-x) - \tan(ct-x))^2}{\frac{6a_2\delta_2(n-1)^2}{\left(16\tau_2^2-1\right)(n+1)(c^2-k^2)} - \frac{4a_2\delta_2\left(2\tau_2-1\right)(n-1)^2(\sec(ct-x)-\tan(ct-x))^2}{\left(16\tau_2^2-1\right)(n+1)(c^2-k^2)}}\right)^{\frac{1}{n-1}}, \tag{42}$$

or

$$\eta_{11,3}(x,t) = \left(\frac{\delta_2\cos^2(ct-x)}{(1-\sin(ct-x))^2\left(\frac{6a_2\delta_2(n-1)^2}{\left(16\tau_2^2-1\right)(n+1)(c^2-k^2)} - \frac{4a_2\delta_2\left(2\tau_2-1\right)(n-1)^2\cos^2(ct-x)}{\left(16\tau_2^2-1\right)(n+1)(c^2-k^2)(1-\sin(ct-x))^2}\right)}\right)^{\frac{1}{n-1}}, \tag{43}$$

are obtained, such that

$$\tau_4^2\left(\frac{1}{2} - \tau_2\right)\left(\frac{9}{16} - \left(\frac{1}{2} - \tau_2\right)\left(\tau_2 + 1\right)\right) + 3\tau_6\left(\tau_2^2 - \frac{1}{16}\right)^2 = 0.$$

12. If $\mathcal{L}_0 = \frac{-\left(1-\alpha^2\right)^2}{4}$, $\mathcal{L}_2 = \frac{1+\alpha^2}{2}$, $\mathcal{L}_4 = \frac{-1}{4}$, $0 < \alpha < 1$, then $Q(\mu) = \alpha cn(\mu,\alpha) \pm dn(\mu,\alpha)$ and resulting in

$$\eta_{12,1}(x,t) = \delta_2\left(\frac{\alpha cn(\mu,\alpha) \pm dn(\mu,\alpha)}{\sqrt{h_1(\alpha cn(\mu,\alpha) \pm dn(\mu,\alpha))^2 + h_2}}\right)^2, \tag{44}$$

where the values of h_1 and h_2 are ascertained by

$$h_1 = -\frac{8\tau_4\left(-2\tau_2 + \alpha^2 + 1\right)}{-16\tau_2^2 + \alpha^4 + 14\alpha^2 + 1},$$
$$h_2 = \frac{12\tau_4\left(\alpha^2 - 1\right)^2}{-16\tau_2^2 + \alpha^4 + 14\alpha^2 + 1},$$

under the constraint condition $\tau_4^2\left(\frac{1}{2}\left(\alpha^2+1\right) - \tau_2\right)\left(\frac{9}{16}\left(1-\alpha^2\right)^2 - \left(\frac{1}{2}\left(\alpha^2+1\right) - \tau_2\right)\left(\tau_2 + \alpha^2 + 1\right)\right) + 3\tau_6\left(\tau_2^2 + \frac{3}{16}\left(1-\alpha^2\right)^2 - \frac{1}{4}\left(\alpha^2+1\right)^2\right)^2 = 0$.

If α tends toward 0, the solution becomes periodic waves (See fig. 13)

$$\eta_{12,1}(x,t) = \left(\frac{\delta_2\cos^2(ct-x)}{-\frac{6a_2\delta_2(n-1)^2}{\left(16\tau_2^2-1\right)(n+1)(c^2-k^2)} - \frac{4a_2\delta_2\left(2\tau_2-1\right)(n-1)^2\cos^2(ct-x)}{\left(16\tau_2^2-1\right)(n+1)(c^2-k^2)}}\right)^{\frac{1}{n-1}}, \tag{45}$$

such that

$$\tau_4^2\left(\frac{1}{2} - \tau_2\right)\left(\frac{9}{16} - \left(\frac{1}{2} - \tau_2\right)\left(\tau_2 + 1\right)\right) + 3\tau_6\left(\tau_2^2 - \frac{1}{16}\right)^2 = 0.$$

13. If $\mathcal{L}_0 = \frac{1}{4}$, $\mathcal{L}_2 = \frac{1-2\alpha^2}{2}$, $\mathcal{L}_4 = \frac{1}{4}$, $0 < \alpha < 1$, then $Q(\mu) = \frac{sn(\mu,\alpha)}{1\pm cn(\mu,\alpha)}$ and resulting in

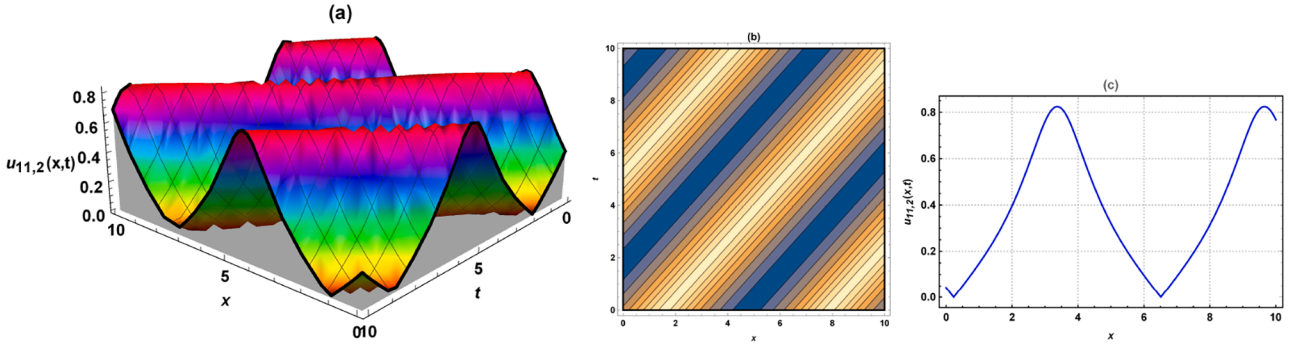


Fig. 11. Visual representation of the solution $\eta_{11,2}(x,t)$ given by Eq. (42) in the limit as $\alpha \to 0$. (a) Three-dimensional profile showing wave propagation, (b) contour plot illustrating the wavefronts, and (c) 2D view at fixed time, highlighting the oscillatory structure. The simulation is performed with the parameter values $c = 0.9,\ n = 3,\ k = 0.8,\ a_2 = 0.2,\ \tau_2 = 0.35$..

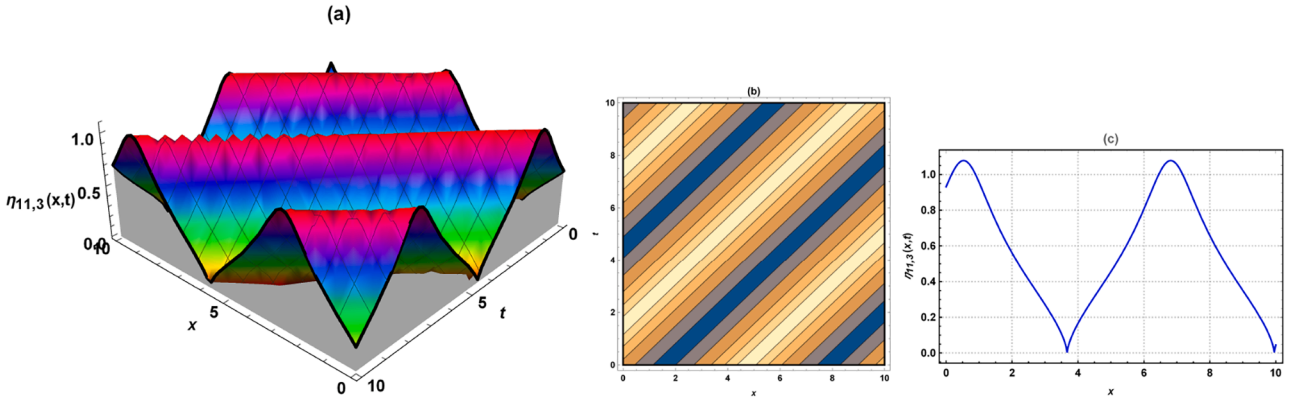


Fig. 12. Visual representation of the solution $\eta_{11,3}(x,t)$ given by Eq. (43) in the limit as $\alpha \to 0$. (a) Three-dimensional profile showing wave propagation, (b) contour plot illustrating the wavefronts, and (c) 2D view at fixed time, highlighting the oscillatory structure. The simulation is performed with the parameter values $c = 1.05,\ n = 4,\ k = 0.8,\ a_2 = 0.4,\ \tau_2 = 0.4$..

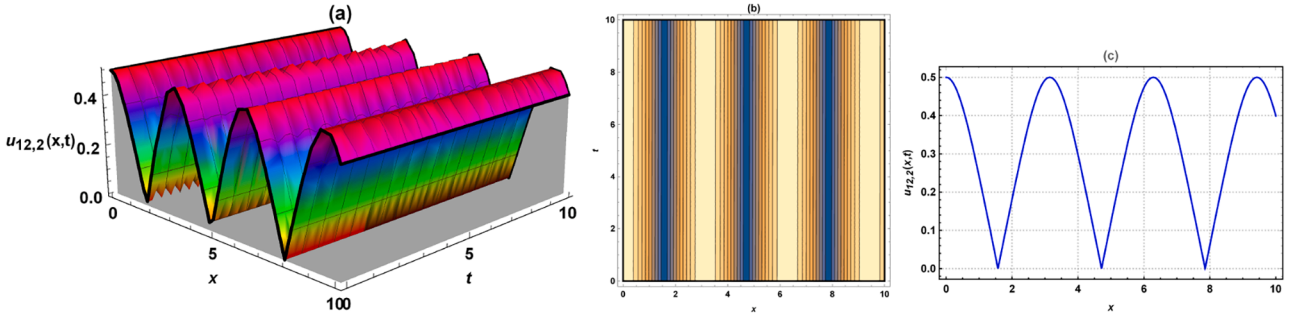


Fig. 13. Visual representation of the solution $\eta_{12,1}(x,t)$ given by Eq. (45) in the limit as $\alpha \to 0$. (a) Three-dimensional profile showing wave propagation, (b) contour plot illustrating the wavefronts, and (c) 2D view at fixed time, highlighting the oscillatory structure. The simulation is performed with the parameter values $c = 0.001,\ n = 3,\ k = 0.5,\ a_2 = 0.1,\ \tau_2 = 0.3$..

$$\eta_{13,1}(x,t) = \delta_2 \left(\frac{\frac{sn(\mu,\alpha)}{1 \pm cn(\mu,\alpha)}}{\sqrt{h_1 \left(\frac{sn(\mu,\alpha)}{1 \pm cn(\mu,\alpha)} \right)^2 + h_2}} \right)^2, \tag{46}$$

where the values of h_1 and h_2 are ascertained by

$$h_1 = \frac{8\tau_4 \left(2\tau_2 + 2\alpha^2 - 1\right)}{-16\tau_2^2 + 16\alpha^4 - 16\alpha^2 + 1},$$

$$h_2 = -\frac{12\tau_4}{-16\tau_2^2 + 16\alpha^4 - 16\alpha^2 + 1},$$

under the constraint condition

$$\tau_4^2 \left(\frac{1}{2}\left(1 - 2\alpha^2\right) - \tau_2 \right) \left(\frac{9}{16} - \left(\frac{1}{2}\left(1 - 2\alpha^2\right) - \tau_2 \right) \left(\tau_2 - 2\alpha^2 + 1 \right) \right) + 3\tau_6 \left(\tau_2^2 - \frac{1}{4}\left(1 - 2\alpha^2\right)^2 + \frac{3}{16} \right)^2 = 0.$$

If $\alpha \to 1$, then the following solution is derived (See fig. 14)

$$\eta_{13,2}(x,t) = \left(\frac{\delta_2 \tanh^2(ct - x)}{(\mathrm{sech}(ct - x) + 1)^2 \left(\frac{6a_2\delta_2(n-1)^2}{\left(16\tau_2^2 - 1\right)(n+1)\left(c^2 - k^2\right)} - \frac{4a_2\delta_2\left(2\tau_2 + 1\right)(n-1)^2 \tanh^2(ct-x)}{\left(16\tau_2^2 - 1\right)(n+1)\left(c^2 - k^2\right)(\mathrm{sech}(ct-x)+1)^2} \right)} \right)^{\frac{1}{n-1}}, \tag{47}$$

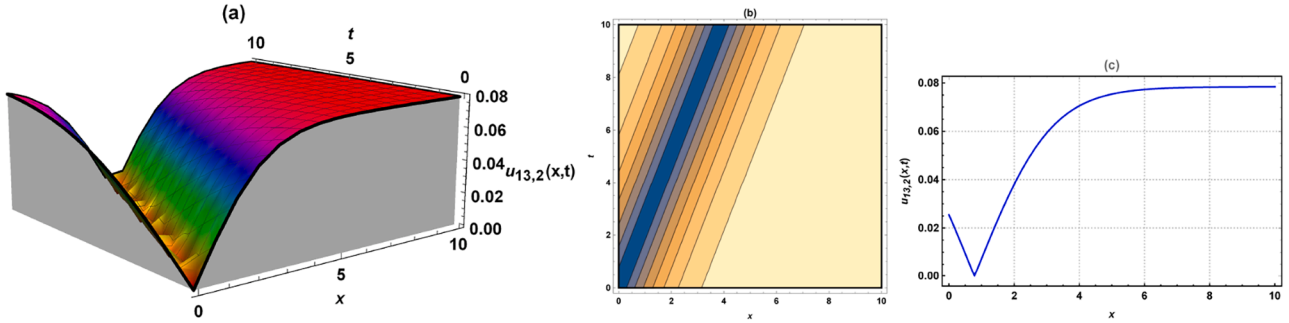


Fig. 14. Visual representation of the solution $\eta_{_{13,2}}(x,t)$ given by Eq. (47) in the limit as $\alpha \to 1$. (a) Three-dimensional profile showing wave propagation, (b) contour plot illustrating the wavefronts, and (c) 2D view at fixed time, highlighting the oscillatory structure. The simulation is performed with the parameter values $c = 0.39,\ n = 3,\ k = 0.3,\ a_2 = 1.01,\ \tau_2 = -0.3$..

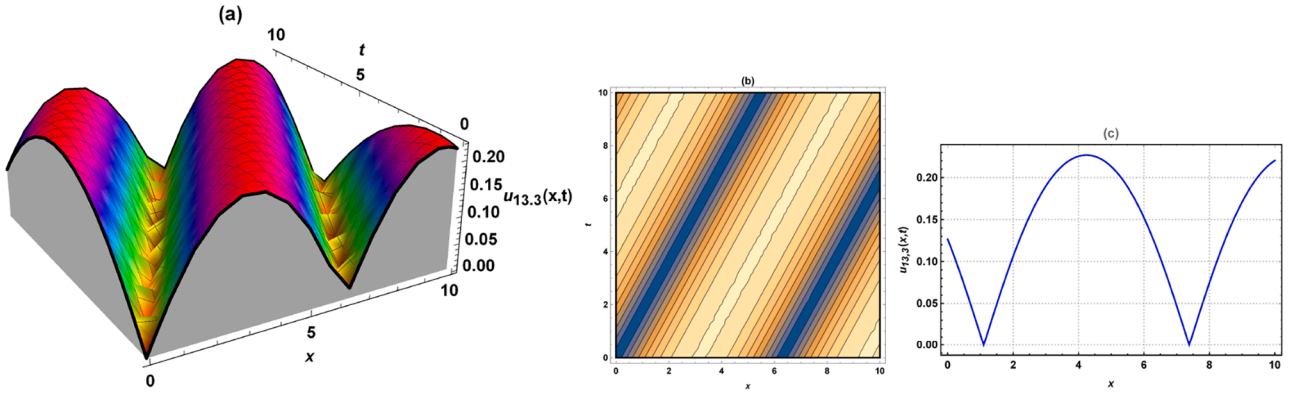


Fig. 15. Visual representation of the solution $\eta_{_{13,3}}(x,t)$ given by Eq. (48) in the limit as $\alpha \to 0$. (a) Three-dimensional profile showing wave propagation, (b) contour plot illustrating the wavefronts, and (c) 2D view at fixed time, highlighting the oscillatory structure. The simulation is performed with the parameter values $c = 0.55,\ n = 3,\ k = 0.4,\ a_2 = 0.6,\ \tau_2 = -0.4$..

such that

$$\tau_4^2\left(-\tau_2-\frac{1}{2}\right)\left(\frac{9}{16}-\left(-\tau_2-\frac{1}{2}\right)(\tau_2-1)\right)+3\tau_6\left(\tau_2^2-\frac{1}{16}\right)^2=0.$$

In the limit as $\alpha \to 0$, the Jacobi elliptic function degenerates into a hyperbolic form, leading to the emergence of a combined periodic wave (See figure 15)

$$\eta_{_{13,3}}(x,t)=\left(\frac{\delta_2\sin^2(ct-x)}{(\cos(ct-x)+1)^2\left(\frac{6a_2\delta_2(n-1)^2}{\left(16\tau_2^2-1\right)(n+1)(c^2-k^2)}-\frac{4a_2\delta_2(2\tau_2-1)(n-1)^2\sin^2(ct-x)}{\left(16\tau_2^2-1\right)(n+1)(c^2-k^2)(\cos(ct-x)+1)^2}\right)}\right)^{\frac{1}{n-1}}, \tag{48}$$

such that

$$\tau_4^2\left(\frac{1}{2}-\tau_2\right)\left(\frac{9}{16}-\left(\frac{1}{2}-\tau_2\right)(\tau_2+1)\right)+3\tau_6\left(\tau_2^2-\frac{1}{16}\right)^2=0.$$

4. Verification of conservation laws in traveling wave solutions of a generalized Klein–Gordon model

In this section, we explicitly verify that the conservation laws derived via Noether'ss Theorem for the generalized nonlinear Klein–Gordon (GNKG) equation hold on its traveling wave solutions. This verification confirms the physical and mathematical significance of these conservation laws in describing wave dynamics.

4.1. The GNKG equation and traveling wave reduction

Consider the GNKG equation for the case $n = 1$:

$$\eta_{tt} - k^2\eta_{xx} + a_1\eta - a_2\eta^2 + a_3\eta^4 = 0,$$

where $\eta = \eta(x,t)$ is the wave field, and a_1, a_2, a_3, k are constants.

We seek traveling wave solutions of the form

$$\eta(x,t) = \phi(\xi), \quad \xi = x - ct,$$

where c is the wave speed and ϕ is a function of the traveling coordinate ξ. Computing derivatives,

$$\eta_t = -c\phi', \quad \eta_{tt} = c^2\phi'', \quad \eta_x = \phi', \quad \eta_{xx} = \phi'',$$

where prime denotes differentiation with respect to ξ. Substitution into the GNKG equation yields an ordinary differential equation (ODE):

$$(c^2 - k^2)\phi'' + a_1\phi - a_2\phi^2 + a_3\phi^4 = 0.$$

4.2. First integral of the traveling wave ODE

Theorem 1. *The traveling wave ODE admits a first integral given by*

$$\frac{1}{2}(c^2-k^2)(\phi')^2 + \frac{a_1}{2}\phi^2 - \frac{a_2}{3}\phi^3 + \frac{a_3}{5}\phi^5 = A,$$

where A is a constant of integration.

Proof. Multiply the ODE by ϕ' and integrate with respect to ξ:

$$(c^2 - k^2)\phi'\phi'' + a_1\phi\phi' - a_2\phi^2\phi' + a_3\phi^4\phi' = 0.$$

Rewrite each term as total derivatives:

$$\frac{d}{d\xi}\left[\frac{1}{2}(c^2-k^2)(\phi')^2 + \frac{a_1}{2}\phi^2 - \frac{a_2}{3}\phi^3 + \frac{a_3}{5}\phi^5\right] = 0.$$

Hence the expression in brackets is a constant, denoted A. For localized solitary wave solutions decaying at infinity, set $A = 0$. □

4.3. Conservation of energy on traveling waves

Theorem 2. *The energy*

$$E = \int_{-\infty}^{\infty} \mathcal{E}(x,t)\,dx,$$

with energy density

$$\mathcal{E}(x,t) = \frac{1}{2}\eta_t^2 + \frac{k^2}{2}\eta_x^2 + \frac{a_1}{2}\eta^2 - \frac{a_2}{3}\eta^3 + \frac{a_3}{5}\eta^5,$$

is conserved in time when evaluated on traveling wave solutions $\eta(x,t) = \phi(x-ct)$.

Proof. Substitute traveling wave expressions:

$$\eta_t = -c\phi', \quad \eta_x = \phi',$$

so the energy density becomes

$$\mathcal{E}(\xi) = \frac{1}{2}c^2(\phi')^2 + \frac{k^2}{2}(\phi')^2 + \frac{a_1}{2}\phi^2 - \frac{a_2}{3}\phi^3 + \frac{a_3}{5}\phi^5.$$

Using the first integral from **Theorem 1**, solve for $(\phi')^2$:

$$(\phi')^2 = \frac{2}{c^2-k^2}\left(-\frac{a_1}{2}\phi^2 + \frac{a_2}{3}\phi^3 - \frac{a_3}{5}\phi^5\right).$$

Plug back into $\mathcal{E}$:

$$\begin{aligned}\mathcal{E}(\xi) &= \frac{c^2+k^2}{2}(\phi')^2 + \frac{a_1}{2}\phi^2 - \frac{a_2}{3}\phi^3 + \frac{a_3}{5}\phi^5 \\ &= \frac{c^2+k^2}{2}\cdot\frac{2}{c^2-k^2}\left(-\frac{a_1}{2}\phi^2 + \frac{a_2}{3}\phi^3 - \frac{a_3}{5}\phi^5\right) + \frac{a_1}{2}\phi^2 - \frac{a_2}{3}\phi^3 + \frac{a_3}{5}\phi^5 \\ &= \left(\frac{c^2+k^2}{c^2-k^2}\right)\left(-\frac{a_1}{2}\phi^2 + \frac{a_2}{3}\phi^3 - \frac{a_3}{5}\phi^5\right) + \frac{a_1}{2}\phi^2 - \frac{a_2}{3}\phi^3 + \frac{a_3}{5}\phi^5.\end{aligned}$$

Because $\phi(\xi)$ is localized, the integral

$$E = \int_{-\infty}^{\infty} \mathcal{E}(\xi)\,d\xi$$

exists and does not depend explicitly on t (since $\xi = x - ct$). Hence,

$$\frac{dE}{dt} = 0,$$

proving energy conservation. □

4.4. Conservation of momentum on traveling waves

Theorem 3. *The momentum*

$$P = \int_{-\infty}^{\infty} \mathcal{P}(x,t)\,dx,$$

with momentum density

$$\mathcal{P}(x,t) = \eta_t\eta_x,$$

is conserved in time on traveling wave solutions.

Proof. Substitute traveling wave expressions:

$$\mathcal{P}(\xi) = \eta_t\eta_x = (-c\phi')(\phi') = -c(\phi')^2.$$

Total momentum:

$$P = -c\int_{-\infty}^{\infty} (\phi')^2\,d\xi,$$

which is a constant independent of time because ϕ is a fixed profile moving with speed c. Therefore,

$$\frac{dP}{dt} = 0,$$

confirming momentum conservation. □

The explicit verification of energy and momentum conservation laws on traveling wave solutions demonstrates: The physical relevance of these laws as conserved quantities that persist in exact, localized wave solutions. The mathematical consistency of the GNKG equation'ss variational and symmetric structure, reflected in the first integral and the conserved densities. The foundation for stability analyses and solitary wave dynamics such as elastic interactions and persistence. The utility of Noether'ss theorem in linking symmetries to tangible conservation laws realized in solution behavior.

We have proven that the conservation laws derived via Noether'ss theorem for the generalized nonlinear Klein–Gordon equation are indeed satisfied on solitary traveling wave solutions. This rigorous verification strengthens the bridge between abstract theoretical frameworks and concrete wave phenomena, underlining the equation'ss suitability for modeling nonlinear wave dynamics.

5. Results and discussion

In this study, the traveling wave solutions of the high-order generalized nonlinear Klein–Gordon equation were analytically investigated using the ϕ^6-expansion method. By applying the traditional traveling wave transformation, the initial nonlinear partial differential equation was reduced to an ordinary differential equation, enabling a systematic analysis of the solution structure. To apply the ϕ^6-expansion method to the reduced equation, the solution was determined by calculating the coefficients based on the principle of balancing the highest-order linear term with the strongest nonlinear term. This approach enabled the systematic derivation of various analytical solution forms under different parameter conditions. The analysis was performed for different nonlinear indices representing physically meaningful nonlinear regimes. As a result of the applied method, various traveling wave solutions expressed in terms of hyperbolic and trigonometric functions have been successfully derived. Among the obtained solutions, different nonlinear wave structures such as singular hyperbolic traveling waves and singular periodic traveling waves have been successfully obtained. The emergence of these solutions depends on the parameter relationships obtained during the application of the method and certain constraint conditions derived from the balancing process. These constraints ensure the mathematical consistency of the solution structure and determine the parameter regions where the obtained wave profiles can exist. Additionally, the accuracy of the obtained solutions has been verified by substituting them back into both the reduced ordinary differential equation and the generalized nonlinear Klein–Gordon equation and checking that the necessary parameter conditions are satisfied. These results analytically reveal the different wave behaviors that may arise in generalized nonlinear Klein–Gordon-type systems and extend existing work in the literature by providing new exact solutions. The findings are expected to contribute to the understanding of nonlinear wave propagation and guide future analytical studies on similar nonlinear evolution equations.

The verified traveling wave solutions reveal various classes of nonlinear wave structures expressed in terms of hyperbolic and trigonometric functions. In particular, traveling wave solutions include singular hyperbolic traveling waves and singular periodic traveling waves. These wave profiles exhibit different qualitative behaviors depending on the model's governing parameters. The existence of singular structures stems from the functional properties of the hyperbolic functions appearing in the solutions, leading to singular points for certain parameter values. Such singular wave patterns can describe nonlinear wave propagation phenomena involving steep gradients or localized singular structures in various physical systems. Numerous analytical methods have been developed in the literature to obtain exact traveling wave solutions for nonlinear Klein–Gordon-type equations. These include the (G'/G)-expansion method (Siddique et al., 2019), the $(G'/G, 1/G)$-expansion method (Zayed and Alurrfi, 2014), the Modified Tanh-Function Expansion Method and a Direct Approach (Alurrfi, 2025), the extended tanh method (Roshid et al., 2021) and various auxiliary equation methods.

These approaches have been successfully applied to obtain soliton, periodic, and singular wave structures for different nonlinear Klein–Gordon models. However, a significant portion of these methods constrain the solution structure to specific functional forms and may complicate the derivation of broader solution families for some nonlinear models. In this context, the ϕ^6-expansion method used in the present study offers a more flexible and systematic solution profile for higher-order nonlinear Klein–Gordon equations. Thanks to this method, some solutions expressed in terms of hyperbolic functions and exhibiting singularities at certain points, known in the literature as singular hyperbolic traveling waves, trigonometric traveling waves, and singular periodic traveling wave solutions, can be obtained, thus enabling the discovery of richer solution families for nonlinear Klein–Gordon type equations. In this respect, the study contributes to obtaining new wave structures for high-order generalized Klein–Gordon models by extending existing analytical studies in the literature.

The ϕ^6-expansion method used in this study provides an effective approach for obtaining analytical solutions to nonlinear evolution equations. The main advantages of the method can be summarized as follows:

- The ϕ^6-expansion method provides access to a broader solution space compared to classical expansion methods, as it is based on expressing the solution as a polynomial expansion in terms of an auxiliary function. This feature enables the derivation of solutions with different wave structures for nonlinear equations.
- The auxiliary equation structure used in the method allows for obtaining different solution forms based on hyperbolic and trigonometric functions. This enables the systematic generation of various traveling wave solutions representing different physical wave behaviors.
- Using a single method, different solution classes such as hyperbolic waves, trigonometric waves, singular waves, and periodic wave solutions, or combinations of these solutions, can be obtained. This demonstrates that the method is quite productive from an analytical perspective.

However, the method also has some limitations.

- If the degree of expansion increases, the algebraic equation systems obtained to determine the coefficients can become quite complex, which can complicate the calculation process.
- Although it has the potential to produce different solutions compared to other analytical methods, the ϕ^6-expansion method may not generate all possible solutions for nonlinear equations and generally produces solution families limited to specified functional forms.

Among the obtained solution families, the traveling wave solution presented by Eq. (36) has been specifically selected for examination. The primary reason for selecting this traveling wave solution is its ability to represent localized wave behavior, which frequently arises in nonlinear Klein–Gordon-type equations due to its structure involving hyperbolic functions. The $sinh(ct - x)$ terms in the solution indicate that the wave profile can exhibit a localized structure in space and time. Hyperbolic functions generally play an important role in nonlinear wave theory in obtaining soliton-like or singular wave solutions. This model, selected to represent the traveling wave solution, may also exhibit amplitude growth or singular behavior under certain parameter conditions due to the hyperbolic function terms in the denominator. Therefore, this solution can be classified as belonging to the singular hyperbolic traveling wave class. Such solutions may represent situations where energy concentration or sharp changes in the wave profile occur in nonlinear wave dynamics. Each parameter included in the model selected for discussion carries a specific physical meaning. These parameters are quantitative quantities representing the physical processes and properties that define the system's behavior, enabling the model to be interpreted in a manner consistent with physical reality. In this context, the parameters used in the model can be defined as follows: c is the propagation speed of the wave, k is the characteristic wave propagation parameter of the medium, a_2 is the coefficient determining the intensity of nonlinear interaction, n is the degree of nonlinear interaction, τ_2 is the parameter affecting the wave profile, and δ_2 is the scale parameter controlling the amplitude of the wave. The relationship between an intrinsic propagation parameter (k), which arises from the physical properties of the medium, and the propagation speed (c) in the space–time plane plays a significant role in determining wave dynamics. In particular, the $c^2 > k^2$ condition emerges as a necessary condition for nonlinear traveling waves to propagate stably through the medium. The solutions obtained under the $c > k$ condition represent physically plausible traveling waves. By assuming all parameters other than the characteristic wave propagation parameter k of the medium to be constant, fig. 16 is obtained to illustrate the spatiotemporal behavior of the solution for different values of k.

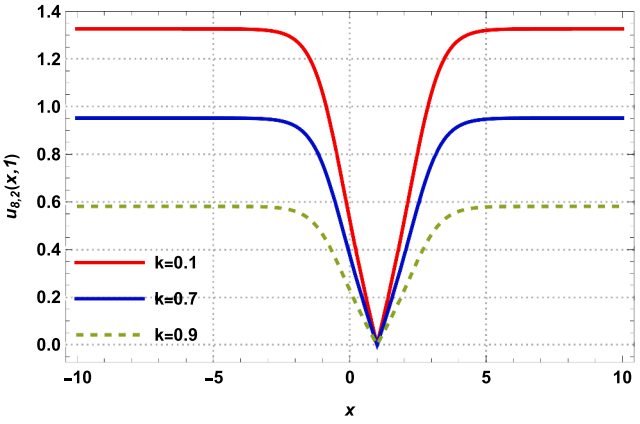


Fig. 16. Visual representation of the solution $\eta_{8,2}(x,t)$ given by Eq. (36) in the limit as $\alpha \to 1$. 2D view at fixed time, highlighting the oscillatory structure. The simulation is performed with the parameter values $c = 1,\ n = 3,\ a_2 = -1.8,\ \tau_2 = 0.6$..

From a physical perspective, the limit $c\beta k$ means that the wave velocity approaches the medium'ss characteristic propagation velocity. In this case, the natural propagation scales of the wave and the medium converge, and the effects of nonlinear interactions become pronounced. Exactly at $c = k$, since the coefficient in the reduced equation approaches zero, the traveling wave reduction may degenerate, and the solution structure may lose its regular traveling wave form. Therefore, to obtain physically meaningful and regular traveling wave solutions, the condition $c > k$ must generally be satisfied. The results of the analysis indicate that as the parameter c approaches the value of k, the system approaches its critical wave propagation regime, and the resulting nonlinear wave solutions may exhibit significant changes in amplitude and structure.

6. Conclusion

In this study, we applied the ϕ^6-expansion method to obtain exact traveling wave solutions of higher-order generalized nonlinear Klein–Gordon equations. The method successfully produced analytical solutions for multiple nonlinearity indices, including solitons, and periodic waveforms, demonstrating its versatility and efficiency. Among the various solution families obtained, we examined the traveling wave solution given by Eq. (36) in detail. This solution, characterized by hyperbolic sine functions, exhibits localized wave behavior representative of soliton-like structures in nonlinear Klein-Gordon systems. In addition, the physical validity of the obtained solutions was evaluated by considering the relationships among the model parameters, and the behavior of the solution was analyzed for different values of the characteristic wave propagation parameter of the medium through which the wave propagates. The results highlight several important points: The ϕ^6-method provides a systematic and straightforward procedure for deriving exact

solutions, often more efficient than traditional methods such as the tanh-function or (G'/G)-expansion techniques. The obtained solutions enrich the theoretical understanding of nonlinear wave propagation in various physical systems, including fluid dynamics, nonlinear optics, and quantum field theory. The study confirms that exact analytical solutions serve as a valuable tool for validating numerical simulations and for exploring interactions between nonlinear waves, such as soliton collisions. Overall, the ϕ^6-expansion method offers a powerful framework for studying nonlinear evolution equations, and the solutions derived in this work can be extended to other nonlinear PDEs with higher-order or variable-coefficient structures (Yagdjian, 2015; Yokuş et al., 2024), paving the way for further analytical and numerical investigations.

Data availability

Data sharing not applicable to this article as no datasets were generated or analysed during the current study.

Ethical Approval

Not applicable.

Funding

Not applicable.

CRediT authorship contribution statement

Asıf Yokus: Methodology, Writing – review & editing, Investigation, Formal analysis, Data curation; **Muhammad Abubakar Isah:** Writing – original draft, Software, Methodology, Investigation, Conceptualization; **Doğan Kaya:** Writing – review & editing, Validation, Supervision, Investigation, Formal analysis.

Declaration of interests

The authors declare that they have no known competing financial interests or personal relationships that could have appeared to influence the work reported in this paper.

References

Ablowitz, M.J., Kaup, D.J., Newell, A.C., Segur, H., 1974. The inverse scattering transform-fourier analysis for nonlinear problems. Stud. Appl. Math. 53, 249–315.
Ali, M.R., 2018. Darboux transformation for soliton solutions of the modified kadomtsev-petviashvili-II equation. Commun. Math. Model. Appl. 3 (3), 28–36.
Alurrfi, K.A., 2025. Exact travelling wave solutions of the nonlinear klein-gordon equation using the modified tanh-function expansion method and a direct approach. Libyan J. Sci. 28 (1).
Arefin, M.A., Zaman, U. H.M., Akbar, M.A., Uddin, M.H., 2025. Assorted soliton solutions to the time-fractional Klein-Gordon equation: A computational study with truncated m-fractional derivative. 9, p. 15.
Davydov, A.S., 1976. Quantum Mechanics. Pergamon Press. Nd ed.
Duran, S., Yokuş, A., Durur, H., 2021a. Surface wave behavior and refraction simulation on the ocean for the fractional Ostrovsky-Benjamin-bona-mahony equation. Mod. Phys. Lett. B 35 (31), 2150477.
Duran, S., Yokuş, A., Durur, H., Kaya, D., 2021b. Refraction simulation of internal solitary waves for the fractional benjamin-ono equation in fluid dynamics. Mod. Phys. Lett. B 35 (26), 2150363.
Fan, E., 2000. Extended tanh-function method and its applications to nonlinear equations. Phys. Lett. A 277, 212–218.
Feshbach, H., Villars, F., 1958. Elementary relativistic wave mechanics of spin 0 and spin 1/2 particles. Rev. Mod. Phys. 30 (1), 24–45.
Ghanbari, B., 2019. Abundant soliton solutions for the Hirota-Maccari equation via the generalized exponential rational function method. Mod. Phys. Lett. B 33 (9).
Gordon, W., 1926. Der comptoneffekt nach der Schrödingerschen theorie. Z. Phys. 40 (1-2), 117.
Greiner, W., 2000. Relativistic Quantum Mechanics. Wave Equations Springer Verlag. Rd ed.
Greiner, W., Müller, B., 1994. Quantum Mechanics: Symmetries. Springer. Nd ed.
Hietarinta, J., 1987. A search for bilinear equations passing hirota'ss three-soliton condition. I. KDV-type bilinear equations. J. Math. Phys. 28 (8), 1732.
Hietarinta, J., 1997. Introduction to the Hirota bilinear Method. Integrability of Nonlinear Systems. Springer, Berlin, Heidelberg.
Hietarinta, J., 2005. Hirota'ss bilinear method and soliton solutions. Phys. AUC 15 (1), 31–37.
Isah, M.A., Muhammad, A., 2025. Propagation of solitons and nonlinear behavior in nonlinear power law fibers. Altay Conf. Proc. Math. 1, 73–94.
Isah, M.A., Yokuş, A., 2026. Seismic Pulse Propagation: Analytical Modeling and Exact Soliton Solutions.
Isah, M.A., Yokus, A., 2025. Isah, i. dark lump collision phenomena to a nonlinear evolution model in harmonic crystals. Part. Diff. Equ. Appl. Math. 14, 101214.
Isah, M.A., Yokus, A., Kaya, D., 2024a. Bilinear neural network method for obtaining the exact analytical solutions to nonlinear evolution equations and its application to kdv. Khayyam J. Math. 10 (2), 228–248.
Isah, M.A., Yokus, A., Kaya, D., 2024b. Exploring the Influence of Layer and Neuron Configurations on Boussinesq Equation Solutions via a Bilinear Neural Network Framework. pp. 1–17.
Iskenderoglu, G., Kaya, D., 2022. Chirped self-similar pulses and envelope solutions for a nonlinear Schrödinger'ss in optical fibers using lie group method. Chaos Soliton. Fract. 162, 112453.
Kaya, D., 2005. An implementation of the adm for generalized one-dimensional Klein-Gordon equation. Appl. Math. Comput. 166, 426–433.
Kudryashov, N.A., Loguinova, N.B., 2008. Extended simplest equation method for nonlinear differential equations. Appl. Math. Comput. 205 (1), 396–402.
Li, J., Zhang, L., 2002. Bifurcations of traveling wave solutions in generalized one-dimensional Klein-Gordon equation. Chaos Soliton. Fract. 14, 581–593.
Podder, A., Arefin, M.A., Akbar, M.A., Uddin, M.H., 2023. A study of the wave dynamics of the space-time fractional nonlinear evolution equations of beta derivative using the improved bernoulli sub-equation function approach. Sci. Rep. 13 (1), 20478.
Podder, A., Arefin, M.A., Ghazwani, H.A., Uddin, M.H., Akbar, M.A., 2025. Dynamical behavior of soliton solutions to the space-time fractional combined kdv-mkdv equation through two robust techniques. Mod. Phys. Lett. B 39 (18), 2550031.
Rajaraman, R., 1982. Solitons and instantons An Introduction to Solitons and Instantons in Quantum Field Theory.
Roshid, M.M., Karim, M.F., Azad, A.K., Rahman, M.M., Sultana, T., 2021. New solitonic and rogue wave solutions of a klein-gordon equation with quadratic nonlinearity. Part. Diff. Equ. Appl. Math. 3, 100036.
Ryabov, P.N., Sinelshchikov, D.I., Kochanov, M.B., 2011. Application of the Kudryashov method for finding exact solutions of the high order nonlinear evolution equations. App. Math. Comp. 218, 3965–3972.
Sakurai, J.J., 1967. Advanced Quantum Mechanics. Addison Wesley.
Siddique, S. T.A., Hossain, M.D., Akbar, M.A., 2019. Exact wave solutions to the (2 1)-dimensional Klein-Gordon equation with special types of nonlinearity. J. Mech. Cont. Math. Sci. 14, 1–20.
Wazwaz, A.M., 2005. The tanh and the sine-cosine methods for compact and noncompact solutions of the nonlinear klein-gordon equation. Appl. Math. Comput. 167 (2), 1179–1195.
Wazwaz, A.M., 2006. Compactons, solitons and periodic solutions for some forms of nonlinear Klein-Gordon equations. Chaos Soliton. Fract. 28 (4), 1005–1013.
Wazwaz, A.M., 2008. New travelling wave solutions to the Boussinesq and the Klein-Gordon equations. Commun. Nonlinear Sci. Numer. Simul. 13 (5), 889–901.
Weinberg, S., 2002. The Quantum Theory of Fields. Vol. I. Cambridge University Press.
Yagdjian, K., 2015. Integral transform approach to solving klein-gordon equation with variable coefficients. Math. Nachr. 288, 2129–2152.
Yokuş, A., Duran, S., Kaya, D., 2024. An expansion method for generating travelling wave solutions for the (2 1)-dimensional Bogoyavlensky-Konopelchenko equation with variable coefficients. Chaos Soliton. Fract. 178, 114316.
Yokus, A., 2011. Solutions of Some Nonlinear Partial Differential Equations and Comparison of Their Solutions. Technical Report. Firat University. Ph.D Diss.
Yokus, A., Isah, M.A., . Stability Analysis and Soliton Solutions of the Nonlinear Evolution Equation by Homoclinic Technique Based on Hirota Bilinear Form. Vol. 2023. IEEE.
Yokus, A., Isah, M.A., 2023. Dynamical behaviors of different wave structures to the Korteweg-de Vries equation with the Hirota bilinear technique. Phys. A 622, 128819.
Yokus, A., Isah, M.A., 2025. Unveiling novel insights: Nonlinear dispersion dynamics of optical solitons through new ϕ^6-model expansion in the klein-gordon equation. Chin. J. Phys. 95, 476–492.
Yokus, A., Isah, M.A., Tuz, M., 2025. Analytical investigation of nonlinear distribution mechanisms in fluid dynamics through the Boiti-Leon-Manna-Pempinelli equation. pp. 1–16.
Zaman, U. H.M., Arefin, M.A., Akbar, M.A., Uddin, M.H., 2023. Study of the soliton propagation of the fractional nonlinear type evolution equation through a novel technique. PLoS ONE 18 (5), 285178.
Zayed, E. M.E., Al-Nowehy, A.G., 2020. New generalized ϕ^6- model expansion method and its applications to the (3 1) dimensional resonant nonlinear Schrödinger equation with parabolic law nonlinearity. Optik 214, 164702.
Zayed, E. M.E., Al-Nowehy, A.G., El-Shater, M., 2018. New ϕ^6-model expansion method and its applications to the resonant nonlinear schrödinger equation with parabolic law nonlinearity. Eur. Phys. J. Plus 133 (10), 417.
Zayed, E. M.E., Alurrfi, K. A.E., 2014. The $(g'/g, 1/g)$-expansion method and its applications for solving two higher order nonlinear evolution equations. Math. Probl. Eng. 2014 (1), 746538.
Zayed, E. M.E., Gepreel, K.A., 2011. The modified (g'/g)-expansion method and its applications to construct exact solutions for nonlinear pdes. Wseas Trans. Math. 10 (8), 270–278.
Zhang, W., Ma, W., 1999. Explicit solitary wave solutions to generalized one-dimensional Klein-Gordon equations. Appl. Math. Mech. 20, 666–674.